UC San Diego
UC San Diego Electronic Theses and Dissertations

Title

The Role of IkappaBalpha and DNA binding in NFkappaB Regulation, Dynamics, and Function

Permalink

Author

Dembinski, Holly Elizabeth

Publication Date

2015

Peer reviewed|Thesis/dissertation

UNIVERSITY OF CALIFORNIA, SAN DIEGO

The Role of IkappaBalpha and DNA binding in
NFkappaB Regulation, Dynamics, and Function

A dissertation submitted in partial satisfaction of the
requirements for the degree of Doctor of Philosophy

in

Chemistry

by

Holly Elizabeth Dembinski

Committee in charge:

      Professor Elizabeth A. Komives, Chair
      Professor Gen-Sheng Feng
      Professor Gourisankar Ghosh
      Professor Partho Ghosh
      Professor Douglas Magde

2015

The dissertation of Holly Elizabeth Dembinski is approved,

and it is acceptable in quality and form for publication on

microfilm:

_____

_____

_____

_____

Chair

University of California, San Diego

2015

Dedication

I dedicate this work to my parents

whose support is unwavering and whose love is unconditional.

Table of Contents

List of Abbreviations

AR	Ankyrin repeat
CD	Circular dichroism
DNA^F	Fluorescein-labeled DNA
DNA^P	Pyrene-labeled DNA
DTT	Dithiothreitol
EDTA	Ethylenediamine triacetic acid
GFP	Green fluorescent protein
H/D	Hydrogen/deuterium
HDX	Hydrogen/deuterium exchange
HDXMS	Hydrogen/deuterium exchange mass spectrometry
HSQC-TROSY	Heteronuclear spin quantum coherence transverse relaxation optimized spectroscopy
IκB	Inhibitor of NFκB
IκBα	IκB isoform alpha
IκBα 5×PEST	IκBα E282Q/E284Q/D285N/E286Q/E287Q
k_a	Association rate
k_d	Dissociation rate
K_D	Dissociation rate constant
NFκB	Nuclear factor kappa B
NMR	Nuclear magnetic resonance
MEF	Mouse embryonic fibroblast
SFF	stopped-flow fluorescence
SPR	Surface plasmon resonance
WT	Wild type

List of Figures

List of Tables

Acknowledgements

I have been blessed with innumerable sources of support throughout my graduate career. To each who has listened, tolerated, and encouraged, to each who has laughed with—and at—me, and to each who has commiserated in failures and rejoiced in successes, you have my sincerest gratitude.

To Prof. Elizabeth A. Komives, PhD—Betsy—thank you for molding me into the protein chemist, biophysicist, and instrument repair specialist I am today. I am persistently in awe of your abilities to remain calm and collected when instruments fail or experiments go awry, to motivate with plenty of carrots—and the occasional stick—to support your students and colleagues as they encounter life's hardships, and to celebrate with students and colleagues as hard-fought successes are won. Thank you for teaching me how to dissemble and repair an HPLC, and a CD, and a UV/Vis, and a Biacore, and a stopped-flow fluorimeter, and an Akta; more importantly, thank you for teaching me how to put everything back together. Thank you for underscoring the importance of little k's, big K's, fresh protein, methodically planned experiments, and the musical stylings of Janis Joplin and Louis Armstrong. Thank you for your patience and your dedication in sharing your craft with me. I hope to make you proud.

To Prof. Stacey Brydges, PhD, thank you for taking me under your wing and introducing me to the field of Chemical Education Research and Practice. Over these past three years, I have come to see in you the instructor I aspire to be. Your dedication to excellence, your investment in your students, and your passion and compassion never cease to amaze me. As I reflect back on my graduate career, I

consider myself immensely blessed to have had the opportunity to work with someone of such expertise, caliber, and elegance. For your mentorship and your friendship, you have my sincerest gratitude. I hope too to make you proud.

Lastly and most importantly, I wish to thank my family. To my parents, I realize I am not the first "Dr. Dembinski," nor do I imagine I will be the last, but I am a "Dr. Dembinski" because of you. As I continue through life, I come realization that I won the family lottery. Thank you for your unwavering support and unconditional love. I will continue to make you proud.

Chapter 2, in full, is material in preparation for journal submission of which the dissertation author was the principal researcher and author. The material will be submitted for publication (**Dembinski, H.**, Wismer, K., Kern, N., Kroon, G., Dyson, H.J., Komives, E.A. Biophysical characterization of the stabilized ternary NFκB-DNA-IκBα complex.)

Chapter 3, in full, is material in preparation for journal submission to which the dissertation author contributed equally with J. Vargas. The material will be submitted for publication (**Dembinski, H.**, Vargas, J., Peacock, R., Wismer, K., Hoffmann, A., Komives, E.A. Functional consequences of IκBα-mediated accelerated dissociation of NFκB from transcription sites).

Chapter 4, in full, is a reprint of which the dissertation author was the principal researcher and author. The material appears in *Physical Chemistry Chemical Physics*. (**Dembinski, H.**, Wismer, K., Balasubramaniam, D., Gonzalez, H., Alverdi, V. Iakoucheva, L.M., Komives, E.A. (2014). Predicted disorder-to-order transition mutations in IκBα disrupt function. *Physical Chemistry Chemical Physics,* **16**, 6480-6485.)

Chapter 5, in full, is material in preparation for journal submission to which the dissertation author contributed equally with K. Ramsey. The material will be submitted for publication (**Dembinski, H.**, Ramsey, K., Komives, E.A. Global stabilization of NFκB upon IκBα and DNA binding).

Vita

2010   Bachelors of Science, Chemistry

Bachelors of Arts, Biology

Bachelors of Arts, French

Gonzaga University, Spokane, WA

2012   Masters of Science, Chemistry

University of California, San Diego, La Jolla, CA

2015   Doctor of Philosophy, Chemistry

University of California, San Diego, La Jolla, CA

Publications

Dembinski, H.; Wismer, K.; Balasubramaniam, D.; Iakoucheva, L.; Komives, E. Predicted disorder-to-order mutations in IκBα disrupt function. *Physical Chemistry Chemical Physics* 2014 (DOI 10.1039/c3cp54427c).

Schwarz, B.H.; Driver, J.; **Dembinski, H.**; Corson, M.H.; Gordon, S.S.; Watson, J.M. Kinetic and bioinformatic characterization of an oxidative, cooperative HMG-CoA reductase from Burkholderia cenocepacia. *Biochemica et Biophysica Acta* 2014 (DOI 10.1016/j.bbapap.2013.11.015).

Lamboy, J.A.; Kim, H.; **Dembinski, H.**; Ha, T.; Komives, E.A. Single-molecule FRET reveals the native-state dynamics of the IκBα ankyrin repeat domain. *Journal of Molecular Biology* 2013 (DOI 10.1016/j.jmb.2013.04.015).

Fields of Study

Major Field: Biochemistry

Studies in Biochemistry and Biophysics

Professor Elizabeth A. Komives

Honors and Awards

2015   Executive Vice Chancellor of Academic Affairs Summer Graduate Teaching Scholar, UC San Diego, La Jolla, CA

2014-2015   Philanthropic Education Organization Dorothy Halleck Education Scholar

2014   K. Patricia Cross Future Leader, UC San Diego Nominee

2014   Protein Society Symposium Best Poster Awardee

2013-2015   Department of Education Graduate Assistance in Areas of National Need Fellow, UC San Diego, La Jolla, CA

2008-2009   Howard Hughes Medical Institute Undergraduate Research Assistant, Gonzaga University, Spokane, WA

Abstract of the Dissertation

The Role of IkappaBalpha and DNA binding in

NFkappaB Regulation, Dynamics, and Function

by

Holly Elizabeth Dembinski

Doctor of Philosophy in Chemistry

University of California, San Diego, 2015

Professor Elizabeth A. Komives, Chair

Nuclear factor kappa B (NFκB) transcription factors are responsible for the regulation of hundreds of target genes, their expression is induced by many classes of stimuli, and NFκBs play essential roles in the healthy regulation of cellular development and proliferation in inflammatory and immune responses. Diseases such as cancer, heart disease, Alzheimer's disease, and AIDS can be attributed to the

aberrant regulation of NFκB. The transcriptional activity of NFκB is controlled by its inhibitors, the IκBs, and IκBα in particular dynamically responds to extracellular stimuli releasing a burst of NFκB that enters the nucleus and activates target genes. The transcriptional activation is short-lived, and our lab is investigating the mechanism of post-induction repression.

After a brief introduction (Chapter 1), I elucidate the role of the IκBα C-terminal PEST sequence in NFκB regulation and biophysically characterize the stabilized NFκB-DNA-IκBα ternary complex (Chapter 2), investigate the importance of IκBα-mediated regulation of NFκB in mouse embryonic fibroblast cells (Chapter 3), probe the coupled folding-upon-binding of IκBα in NFκB regulation (Chapter 4), and explore effect of DNA binding on NFκB stability and dynamics (Chapter 5). These studies suggest that the binding of IκBα and DNA to NFκB have widespread and powerful consequences on NFκB dynamics, function, and regulation.

Chapter 1

Introduction

The NFκB pathway is regulated by IκBs

The Nuclear factor kappa B (NFκB) signaling pathway is responsible for receiving extra-cellular signals, choreographing an intracellular response, and amplifying appropriate intercellular signals. The pathway is integral to healthy cellular functions including cell growth and proliferation, stress response, and apoptosis.[1] Aberrant regulation of NFκB is implicated in innumerable disease states including chronic inflammation, HIV/AIDS, cancer, and Alzheimer's.[2, 3]

The pathway is named after the Nuclear factor kappa B (NFκB), originally discovered in activated B-cells to upregulate expression of the immunoglobulin kappa-chain gene.[4] NFκB is comprised of a family of proteins that form homo- and hetero-dimers of p50, p52, p65 (RelA), RelB, and c-Rel.[2] Inhibitors of NFκB (IκBs) include IκBα, IκBβ, IκBβ, and IκBε, which are responsible for blocking the nuclear localization and transcriptional activity of p65- and c-Rel-containing NFκBs.[5] In resting cells, most of the estimated 100,000 NFκB dimers are sequestered to the cytoplasm by IκBs, thereby minimizing association with DNA.[6, 7]

The NFκB pathway is activated by a variety of extracellular signals (e.g., lipopolysacchardies, double-stranded RNA), as well as innate cytokines, which results in the assembly of the IκB kinase (IKK).[8] IKK phosphorylates NFκB-bound IκBα at the N-terminal signal response domain, resulting in consequent ubiquitination and degradation by the proteasome.[9] Unhindered by IκB cytosolic sequestration, NFκB dimers translocate to the nucleus, bind to κB DNA binding sites, and upregulate downstream genes.[10] The vast number of genes regulated by NFκB have varying

transcription levels, activation kinetics, and post-induction repression,[11, 12] and one of the genes activated by NFκB encodes IκBα.[13-15] Newly synthesized IκBα translocates to the nucleus, binds to NFκB, accelerates its dissociation from DNA, and results in the export of the NFκB-IκBα complex from the nucleus (Figure 1.1).[1, 16, 17] Degradation of free IκBα is ubiquitin-independent yet proteasome-dependent and is extremely rapid ($t_{half-life} < 10$ min); conversely, NFκB-bound IκBα is extraordinarily stable ($t_{half-life} > 12$ h) and is only degraded if phosphorylated, ubiquitinated, and degraded by the proteasome.[1, 18]
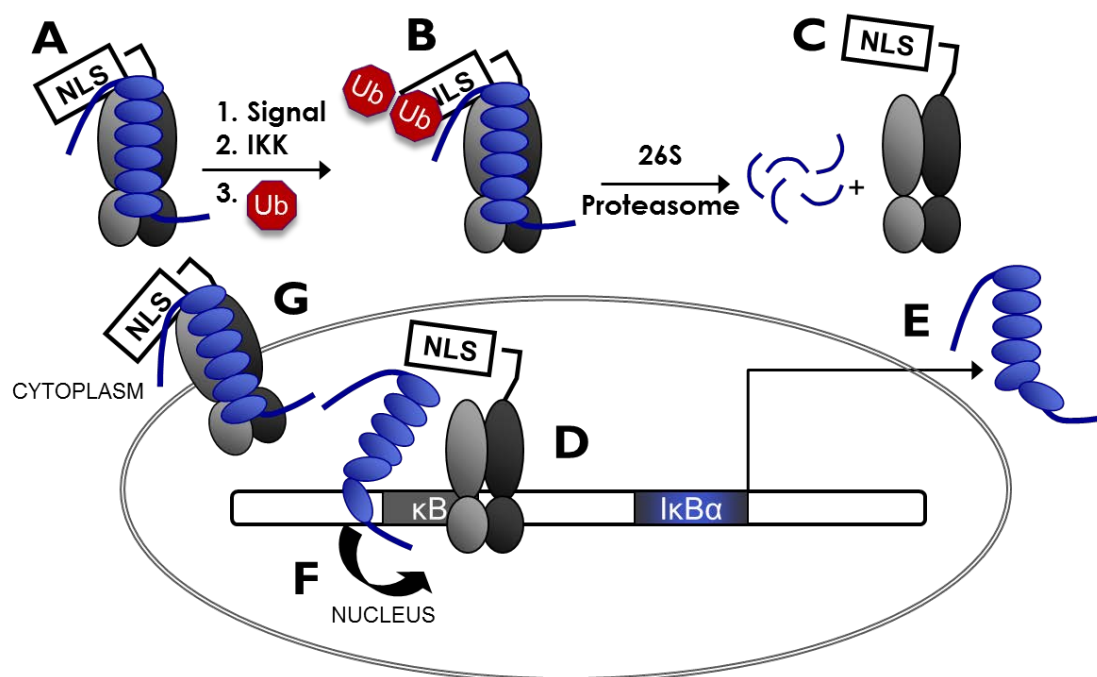
Figure 1.1. IκBα regulates NFκB activity. (A) In resting cells, NFκB is sequestered to the cytoplasm by IκBα. (B) When the NFκB pathway is activated, IκBα is phosphorylated, ubiquitinated, and degraded by the 26S proteasome, leaving the nuclear localization signal (NLS) of NFκB unmasked (C). (D) NFκB can then enter the nucleus and bind to κB promoter sites, one of which regulates IκBα. (E) Newly synthesized IκBα can then enter the nucleus and mediate the dissociation of NFκB from DNA (F), resulting in the export of NFκB out of the nucleus (G).

Structure, folding, dynamics, and function of IκBα

Full-length IκBα protein is composed of three domains: (1) the N-terminal signal response domain, which is the site of phosphorylation and ubiquitination, (2) six ankyrin repeats (ARs) that comprise the AR domain, and (3) a highly acidic, C-terminal PEST sequence (Figure 1.2).[17,18] PEST sequences are rich in proline (P), glutamate (E), serine (S), and threonine (T) residues, are often negatively charged (e.g., acidic and phosphorylated residues), and have been implicated as a protein degradation motif.[19] Both the PEST sequence and AR(5-6) have been shown to be disordered in free IκBα,[20] and these two regions are responsible for IκBα's binding activity to NFκB. The two high resolution crystal structures of the IκBα-NFκB complex show that the AR domain folds as an elongated stack of six ARs (Figure 1.3). IκBα has resisted all attempts to crystallize in the unbound state, and its biophysical behavior is consistent with a native state that does not adopt a compact fold.[21]

```
Consensus      - G - T P L H L A - - - G - - - - V - - L L - - G A - - - - -

Signal
Response    1   M F Q A A E R P Q E W A M E G P R D G L K K E R H D S G L D S

           37   M K D E E Y E Q M V K E L Q E I R L E P Q E V P R G S E P W K Q Q L T E

AR1        73   D G D S F L H L A I I H E E K A L T M E V I R Q V K G D L A F L N F Q N N

AR 2      110   L Q Q T P L H L A V I T N Q P E I A E A L L G A G C D P E L R D F

AR3       143   R G N T P L H L A C E Q G C L A S V G V L T Q S C T T P H L H S I L K A T N Y

AR 4      182   N G H T C L H L A S I H G Y L G I V E L L V S L G A D V N A Q E P C

AR 5      216   N G R T A L H L A V D L Q N P D L V S L L L K C G A D V N R V T Y

AR 6      249   Q G Y S P Y Q L T W G R P S T R I Q Q Q L G Q L T L E N L Q M L

PEST      281   P E S E D E E S Y D T E S E F T E F T E D E L P Y D D C V F G G Q R L T L
```

Figure 1.2. Human IκBα(1-317) sequence aligned with the ankryin repeat consensus sequence. The N-terminal signal response domain (gray), the well-folded AR(1-4) (blue), the intrinsically disordered AR5 and AR6 (purple), and the C-terminal PEST sequence (pink/gray) are highlighted here. Note that the IκBα structure in Figure 2.3 displays only sequence residues in color; gray residues are not shown on the structure.
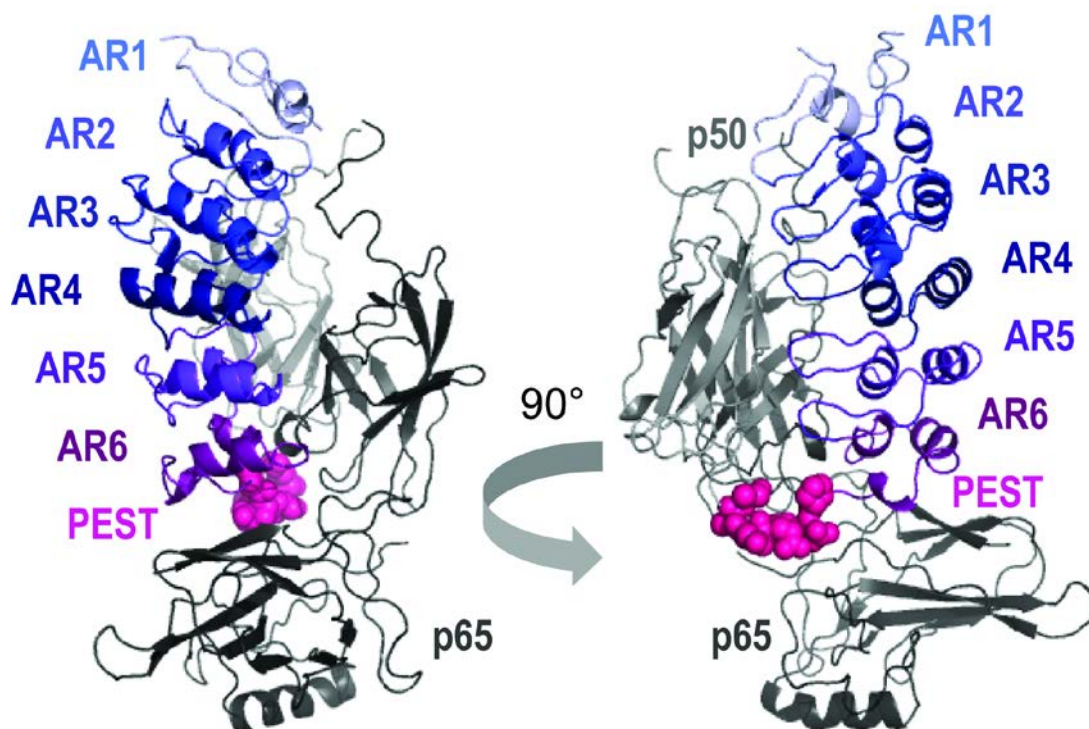
Figure 1.3. IκBα-p50/p65 structure (1IKN). The well-folded IκBα AR(1-4), the intrinsically disordered IκBα AR(5-6) (purple), the IκBα C-terminal PEST sequence (pink), the NFκB p65 subunit (dark gray), and the NFκB p50 subunit (light gray) are shown here.

Alignment of the many hundreds of AR sequences helped to define a consensus sequence (Figure 1.1), and AR domains that are designed with this consensus in mind are highly stable.[22] We noticed that the more consensus-like ARs of IκBα are AR(1-4), and in hydrogen-deuterium exchange mass spectrometry experiments, AR(1-4) had the least amide exchange, whereas AR(5-6) undergo rapid exchange in agreement with the decreased AR consensus sequence conservation.[23, 24]

IκBα has a high affinity for NFκB, resulting from an extremely slow dissociation rate,[7] which is due in part to the coupled folding and binding of the AR(5-6) region.[25] IκBα inhibits the transcriptional activity of NFκB, and we recently showed

that IκBα is remarkably efficient at increasing the dissociation rate (k_d) of NFκB from the DNA; the apparent second order rate constant for the IκBα-mediated dissociation of NFκB from DNA is 10^6 M^{-1} s^{-1}. This process requires that the AR(5-6) region of IκBα be disordered;[26] indeed, introduction of two mutations to the consensus sequence in AR6, Y254L and T257A, resulted in "pre-folding" AR6 such that all six ARs became part of the cooperatively folding AR domain.[27] This mutant had impaired NFκB binding affinity and was also less efficient at dissociating NFκB from DNA.[26, 27] Thus, an important function of the "weakly-folded" region of IκBα may be to facilitate dissociation of NFκB from the DNA to rapidly repress post-induction transcriptional activation.

Toward understanding the role of IκBα and DNA binding in NFκB regulation, dynamics, and function

My thesis work focusses on elucidating the role of IκBα and DNA binding in NFκB regulation, dynamics, and function. I used several solution biophysical approaches including stopped flow fluorescence, fluorescence anisotropy, surface plasmon resonance, circular dichroism, and amide hydrogen/deuterium exchange to more deeply probe the backbone dynamics, binding kinetics, and thermodynamics of IκBα and NFκB as they undergo molecular interactions.

To more fully understand the NFκB-IκBα-DNA interaction, I generated an IκBα mutant that exhibits approximate IκBα WT affinity for NFκB but is unable to mediate the dissociation of NFκB from DNA; in studying this mutant we gained insight into the mechanisms of (1) the IκBα-mediated dissociation of NFκB from

DNA and (2) the formation of the encounter NFκB-DNA-IκBα ternary complex. To probe the importance of IκBα in NFκB regulation, I collaborated with the Hoffmann Lab to employ this mutant in mouse embryonic fibroblast cells (MEFs) and monitor the changes in NFκB activity in MEFs deficient in active IκBα. Together we measured the rate of translocation of NFκB from the nucleus when either wild type or mutant IκBα is present.

Given that IκBα accelerates the dissociation of NFκB from DNA, and this IκBα activity is correlated with the coupled folding-upon-binding, I turned to disorder-to-order mutations of IκBα predicted *in silico* and independently of the consensus design to assess the effects of non-consensus, pre-folding mutations on IκBα activity.

Finally, I explored how the backbone dynamics of NFκB are altered upon DNA binding, paving the way for a more comprehensive analysis of NFκB dynamics throughout the regulatory process.

References

1. Hoffmann, A., Levchenko, A., Scott, M. L., and Baltimore, D. (2002) The IkappaB-NF-kappaB signaling module: temporal control and selective gene activation, *Science 298*, 1241-1245.

2. Ghosh, S., May, M. J., and Kopp, E. B. (1998) NF-kappa B and Rel proteins: evolutionarily conserved mediators of immune responses, *Annu. Rev. Immunol. 16*, 225-260.

3. Kumar, A., Takada, Y., Boriek, A. M., and Aggarwal, B. B. (2004) Nuclear factor-kappaB: its role in health and disease, *J. Mol. Med. 82*, 434-448.

4. Hoffmann, A., and Baltimore, D. (2006) Circuitry of nuclear factor kappaB signaling., *Immunol Rev. 210*, 171-186.

5. Verma, I. M., Stevenson, J. K., Schwarz, E. M., Van Antwerp, D., and Miyamoto, S. (1995) Rel/NF-kappa B/I kappa B family: intimate tales of association and dissociation, *Genes Dev 9*, 2723-2735.

6. Baeuerle, P. A. (1998) IkB-NF-kB structures: at the interface of inflammation control, *Cell 95*, 729-731.

7. Bergqvist, S., Croy, C. H., Kjaergaard, M., Huxford, T., Ghosh, G., and Komives, E. A. (2006) Thermodynamics reveal that helix four in the NLS of NF-kappaB p65 anchors IkappaBalpha, forming a very stable complex, *J. Mol. Biol. 360*, 421-434.

8. Oeckinghaus, A., and Ghosh, S. (2012) The NFkB Family of Transcription Factors and Its Regulation, *Cold Spring Harb. Symp. Perspect. Biol. 1*, 1-14.

9. Traenckner, E. B., and Baeuerle, P. A. (1995) Appearance of apparently ubiquitin-conjugated I kappa B-alpha during its phosphorylation-induced degradation in intact cells, *J. Cell. Sci. Suppl. 19*, 79-84.

10. Pahl, H. L. (1999) Activators and target genes of Rel/NF-kappaB transcription factors, *Oncogene 18*, 6853-6866.

11. Hoffmann, A., Leung, T. H., and Baltimore, D. (2003) Genetic analysis of NF-kappaB/Rel transcription factors defines functional specificities., *EMBO J. 22*, 5530-5539.

12. Werner, S. L., Barken, D., and Hoffmann, A. (2005) Stimulus specificity of gene expression programs determined by temporal control of IKK activity., *Science 309*, 1857-1861.

13. Brown, K., Park, S., Kanno, T., Franzoso, G., and Siebenlist, U. (1993) Mutual regulation of the transcriptional activator NF-kappa B and its inhibitor, I kappa B-alpha, *Proc. Natl. Acad. Sci. U. S. A. 90*, 2532-2536.

14. Scott, M. L., Fujita, T., Liou, H. C., Nolan, G. P., and Baltimore, D. (1993) The p65 subunit of NF-kappa B regulates I kappa B by two distinct mechanisms, *Genes Dev. 7*, 1266-1276.

15. Sun, S. C., Ganchi, P. A., Ballard, D. W., and Greene, W. C. (1993) NF-kappa B controls expression of inhibitor I kappa B alpha: evidence for an inducible autoregulatory pathway, *Science 259*, 1912-1915.

16. Arenzana-Seisdedos, F., Turpin, P., Rodriguez, M., Thomas, D., T., H. R., Virelizier, J.-L., and Dargemont, C. (1997) Nuclear localization of IkBa promotes active transport of NF-kB from the nucleus to the cytoplasm, *J. Cell. Sci. 110*, 369-378.

17. Bergqvist, S., Alverdi, V., Mengel, B., Hoffmann, A., Ghosh, G., and Komives, E. A. (2009) Kinetic enhancement of NF-kappaB•DNA dissociation by IkappaBalpha, *Proc. Nat. Acad. Sci. U.S.A. 106*, 19328-19333.

18. O'Dea, E. L., Barken, D., Peralta, R. Q., Tran, K. T., Werner, S. L., Kearns, J. D., Levchenko, A., and Hoffmann, A. (2007) A homeostatic model of IkappaB metabolism to control constitutive NF-kappaB activity, *Molecular systems biology 3*, 111.

19. Rogers, S., Wells, R., and Rechsteiner, M. (1986) Amino acid sequences common to rapidly degraded proteins: the PEST hypothesis., *Science 234*, 364-368.

20. Garner, E., Romero, P., Dunker, A. K., Brown, C., and Obradovic, Z. (1999) Predicting Binding Regions within Disordered Proteins, *Genome Informatics 10*, 41-50.

21. Croy, C. H., Bergqvist, S., Huxford, T., Ghosh, G., and Komives, E. A. (2004) Biophysical characterization of the free IkappaBalpha ankyrin repeat domain in solution, *Protein Sci 13*, 1767-1777.

22. Binz, H. K., Stumpp, M. T., Forrer, P., Amstutz, P., and Pluckthun, A. (2003) Designing repeat proteins: well-expressed, soluble and stable proteins from combinatorial libraries of consensus ankyrin repeat proteins, *J Mol Biol 332*, 489-503.

23. Croy, C. H., Bergqvist, S., Huxford, T., Ghosh, G., and Komives, E. A. (2004) Biophysical characterization of the free IkappaBalpha ankyrin repeat domain in solution., *Protein Sci. 13*, 1767-1777.

24. Brown, C. J., Johnson, A. K., and Daughdrill, G. W. (2010) Comparing models of evolution for ordered and disordered proteins, *Mol Biol Evol 27*, 609-621.

25. Truhlar, S. M., Torpey, J. W., and Komives, E. A. (2006) Regions of IkappaBalpha that are critical for its inhibition of NF-kappaB.DNA interaction fold upon binding to NF-kappaB, *Proceedings of the National Academy of Sciences of the United States of America 103*, 18951-18956.

26. Bergqvist, S., Alverdi, V., Mengel, B., Hoffmann, A., Ghosh, G., and Komives, E. A. (2009) Kinetic enhancement of NF-kappaBxDNA dissociation by IkappaBalpha, *Proceedings of the National Academy of Sciences of the United States of America 106*, 19328-19333.

27. Truhlar, S. M., Mathes, E., Cervantes, C. F., Ghosh, G., and Komives, E. A. (2008) Pre-folding IkappaBalpha alters control of NF-kappaB signaling, *J Mol Biol 380*, 67-82.

Chapter 2

Biophysical Characterization of the Stable NFκB-DNA-IκBα Ternary Complex

Introduction

Almost 10 years ago, our lab obtained binding kinetic data that showed IκBα dramatically increases the rate of dissociation of NFκB from DNA.[1] More recently, our lab obtained evidence of formation of a transient NFκB-DNA-IκBα ternary complex ternary complex during this dissociation process using stopped-flow fluorescence (SFF).[2] It has been shown that the acidic IκBα PEST residues contact Arg residues in the DNA-binding loops of NFκB,[3] suggesting there may be a mutual exclusivity between binding of the negatively charged PEST sequence and DNA binding to NFκB. Additionally, the truncation of the PEST sequence abrogates IκBα binding affinity for NFκB, rendering PEST truncation an inviable method to stabilize the NFκB-DNA-IκBα ternary complex.[4]

In an effort to stabilize the transient ternary complex, we conservatively mutated the acidic PEST residues to their amide counterparts to generate the IκBα$_{67-287}$ E282Q/E284Q/D285N/E286Q/E287Q (IκBα 5×PEST) mutant (pink residues in Figure 1.2). In the present work, we describe the biophysical characterization of the stabilized NFκB-DNA-IκBα ternary complex by means of fluorescence kinetic measurements, steady-state fluorescence anisotropy, surface plasmon resonance (SPR), heteronuclear spin quantum coherence transverse relaxation optimized spectroscopy (HSQC-TROSY) nuclear magnetic resonance (NMR), and hydrogen-deuterium exchange mass spectrometry (HDX-MS).

Materials and Methods

Protein expression and purification

Human wild-type IκBα$_{67-287}$ (IκBα) and the IκBα mutants E282Q/E284Q/D285N/E286Q/E287Q (5×PEST), E282Q, E284Q, D285N, E286Q, and E287Q were expressed in *E. coli* BL21 DE3 cells and purified using a Hi-Load Q Sepharose column (GE Healthcare, Pittsburgh, PA, USA) followed by a Superdex 75 column (GE Healthcare) as described previously.[5, 6]

^{2}H^{15}N-labeled IκBα WT and IκBα 5×PEST were expressed in *E. coli* BL21 DE3 cells grown in M9 minimal medium in D$_2$O supplemented with ^{15}NH$_4$Cl (2 g/L) as described previously.[7]

Murine, N-terminal hexahistidine-p50$_{39-350}$/RelA$_{19-321}$ heterodimer (NFκB) was co-expressed as described previously[8] and purified by nickel affinity chromatography (Ni-NTA Agarose, Qiagen, Valencia, CA, USA), cation exchange chromatography (Mono S column, GE Healthcare), and size exclusion chromatography (Superdex 200, GE Healthcare).

Hereafter referred to as p50dd/biotin-p65dd, murine dimerization domain RelA$_{190-321}$ with an N-terminal Cys and dimerization domain p50$_{248-350}$ and were expressed, purified, and prepared for surface plasmon resonance as described.[5, 9]

Protein concentrations were determined by spectrophotometry at 280 nm (NFκB ε = 43760 M^{-1} cm^{-1}, IκBα ε = 12950 M^{-1} cm^{-1}). Unless otherwise noted, experiments were performed with proteins in 25 mM Tris pH 7.5, 150 mM NaCl, 1 mM DTT, 0.5 mM EDTA.

DNA labeling and purification

A hairpin DNA sequence corresponding to the IFN-κB site 5'-AmMC6/GGGAAATTCCTCCCCCAGGAATTTCCC-3' (IDT Technologies, Coranville, CT, USA) was labeled with pyrene (N-hydroxyl succinimide ester) (DNA^P) or fluorescein (fluorescein isothiocyanate) (DNA^F) as described.[10]

Stopped-flow fluorescence

SFF experiments were performed on an SX-20 stop-flow apparatus (Applied Photophysics, Leatherhead, UK) at 25 °C set to collect 2000 pt linearly with a final mixing volume of 200 µL. The IκBα-mediated dissociation of DNA^P from NFκB was monitored by adding different concentrations of IκBα WT (0.25, 0.50, 0.75, 1.00, 1.25, 1.50, 1.75, and 2.00 µM) to a 1.00 µM NFκB-1.20 µM DNA^P complex monitoring the change in fluorescence of the pyrene-labeled DNA. The pyrene was excited at 343 nm, and the fluorescence emission was monitored at 376 nm with a cut-off filter at 350 nm. The association of IκBα to NFκB or NFκB-DNA was monitored via the native Trp fluorescence of a single Trp at position 258 in IκBα by exciting at 280 nm and monitoring the emission at 345-355 nm with a cut-off filter at 320 nm. Various concentrations of NFκB or NFκB-DNA (0.30, 0.40, 0.50, 0.60, 0.70, 0.80 µM) were mixed with IκBα (0.10 µM). Data were collected and analyzed as described.[9]

Surface plasmon resonance experiments

Sensorgrams were recorded on a Biacore 3000 instrument using streptavidin chips (GE Healthcare) by immobilizing 150, 250, 350 RU of p50dd/biotin-p65dd on flow cells 2, 3, and 4, respectively, leaving flow cell 1 unmodified for reference subtraction. NFκB binding experiments were conducted on IκBα WT, E282Q, E284Q, D285N, E286Q, E287Q, and 5×PEST, and the data were analyzed as described.[4, 9]

Fluorescence anisotropy

Fluorescence anisotropy data were collected in triplicate on a Beckman Coulter DTX 880 Multimode Detector by exciting fluorescein-labeled DNA at 495 nm and monitoring emission at 519 nm. DNA^F (10 nM) and NFκB (200 nM) were incubated overnight. The NFκB-DNA complex (100 µL) was added to 100 µL IκBα WT or IκBα 5x PEST at final IκBα concentrations of 0, 10, 25, 50, 75, 100, 250, 500, 750, 1000, 1250, and 1500 nM and incubated 1 h at 25 °C prior to data collection. Anisotropy values were calculated according to the equation $r = [I_{(V,V)} - GI_{(V,H)}]/[I_{(V,V)} - 2GI_{(V,H)}]$, where r is anisotropy, $I_{(V,V)}$ is the fluorescence intensity in the parallel direction, $I_{(V,H)}$ is the fluorescence intensity in the perpendicular direction, and G is 0.67, a correction factor for the difference in detection sensitivity for parallel and perpendicular polarized light.[11] Fluorescence anisotropy values reported here were corrected for the anisotropy signal due to free DNA^F.

Nuclear magnetic resonance

NFκB was incubated in a 1.2-fold excess of ^{2}H^{15}N IκBα WT or ^{2}H^{15}N IκBα 5×PEST, and the binary complexes were purified by size exclusion chromatography (Superdex 200, GE Healthcare). For the ternary NFκB-DNA-^{2}H^{15}N IκBα 5×PEST complex, NFκB was incubated in a 1.2 excess of DNA, and ^{2}H^{15}N IκBα 5×PEST was added to the NFκB-DNA complex equimolar to the concentration of NFκB. NMR samples were exchanged into NMR buffer (25 mM D-Tris pH 7.5, 50 mM NaCl, 1 mM EDTA, 1 mM DTT, 90% H$_2$O, 10% D$_2$O) via PD-10 desalting columns (GE Healthcare) and concentrated to 0.12 mM using polyethersulfone Vivaspin 6 concentrators (Sartorius). HSQC-TROSY spectra were collected at 30 °C on a Bruker Avance 800 MHz spectrometer equipped with a cryoprobe with 256 scans and 2048 (t2) × 128 (t1).

The NFκB-^{2}H^{15}N IκBα WT complex had previously been assigned,[8] and these assignments were used to assign the nearly identical HSQC-TROSY spectra of the NFκB-^{2}H^{15}N IκBα 5×PEST complex and the NFκB-DNA-^{2}H^{15}N IκBα 5×PEST. Assignments of the four IκBα 5×PEST mutant residues that remained unassigned, E282Q, E284Q, D285N, E286Q, in the NFκB-^{2}H^{15}N IκBα 5×PEST and NFκB-DNA-^{2}H^{15}N IκBα 5×PEST spectra were made by comparison to the chemical shifts in the corresponding wild type spectra.

Hydrogen-deuterium exchange mass spectrometry

Hydrogen/deuterium exchange mass spectrometry (HDXMS) was performed using Waters nanoACQUITY UPLC system with H/DX technology. The NFκB-DNA-IκBα WT and NFκB-DNA-IκBα 5×PEST samples were prepared by an overnight incubation of NFκB in a ten-fold excess of the aforementioned, unmodified IFN-κB hairpin DNA followed by the addition of IκBα WT or IκBα 5×PEST. The final concentrations were as follows: NFκB (5 µM):DNA (50 µM):IκBα WT (5 µM) or NFκB (5 µM):DNA (50 µM):IκBα 5xPEST (5 µM). For each deuteration time, 4 µL complex was equilibrated to 25 °C for 5 min and then mixed with 565 µL D_2O buffer (25 mM Tris pH 7.5, 150 mM NaCl, 1 mM DTT, 0.5 mM EDTA in D_2O) for 0, 0.5, 1, 2, 5, or 10 min. The exchange was quenched with an equal volume of quench solution (3 M guanidine, 0.1% formic acid, pH 2.66). The quenched sample was then injected into the 50 µL sample loop, followed by digestion on an in-line pepsin column (immobilized pepsin, Pierce, Inc.) at 15°C. The resulting peptides were captured on a BEH C18 Vanguard pre-column, separated by analytical chromatography (Acquity UPLC BEH C18, 1.7 µM, 1.0 X 50 mm, Waters Corporation) using a 7-85% acetonitrile in 0.1% formic acid over 7.5 min, and electrosprayed into the Waters SYNAPT G2Si quadrupole time-of-flight mass spectrometer. The mass spectrometer was set to collect data in the Mobility, ESI+ mode; mass acquisition range of 200–2,000 (m/z); scan time 0.4 s. Continuous lock mass correction was accomplished with infusion of leu-enkephalin (m/z = 556.277) every 30 s (mass accuracy of 1 ppm for calibration standard). For peptide

identification, the mass spectrometer was set to collect data in MS^E, ESI+ mode instead. The peptides were identified from triplicate analyses of 10 μM IκBα WT or IκBα 5×PEST, and data were analyzed using PLGS 2.5 (Waters Corporation). Peptides masses were identified using a minimum number of 250 ion counts for low energy peptides and 50 ion counts for their fragment ions; the peptides also had to be larger than 1500 Da. The following cut-offs were used to filter peptide sequence matches: minimum products per amino acid of 0.2, minimum score of 8, maximum MH+ error of 3 ppm, a retention time standard deviation of 5%, and the peptides had to be present in all three ID runs. The peptides identified in PLGS were then analyzed in DynamX 3.0 (Waters Corporation). The relative deuterium uptake for each peptide was calculated by comparing the centroids of the mass envelopes of the deuterated samples with the undeuterated controls following previously published methods.[12]

Results

IκBα 5×PEST mutant forms a ternary NFκB-DNA-IκBα complex

We compared the IκBα-mediated stripping of NFκB from DNA by SFF using IκBα WT and the IκBα 5×PEST mutant (Figure 2.1A). It has been demonstrated that a pyrene-labeled IFNκB hairpin DNA oligo exhibits increased fluorescence upon binding to NFκB, and when IκBα strips NFκB from DNA^P, a decrease in fluorescence signal is observed.[1] IκBα WT stripped NFκB from DNA^P, restoring the fluorescence signal to that of free DNA^P; however, the IκBα 5×PEST mutant did not strip NFκB from DNA^P to the fluorescence signal of free DNA^P, suggesting that some of the DNA^P remained bound. If the stripping capacity of the IκBα 5×PEST mutant were diminished but not abolished, adding an excess of IκBα 5×PEST to the stripping reaction would result in decreased fluorescence signal, reflective of free DNA^P; however, when we added a twenty-fold excess of IκBα 5×PEST, the rate of the reaction increased, but the change in amplitude in the SFF trace remained constant (Figure 2.1B). These data suggest that the IκBα 5×PEST mutant did not strip NFκB from DNA^P and that the DNA^P remained bound.
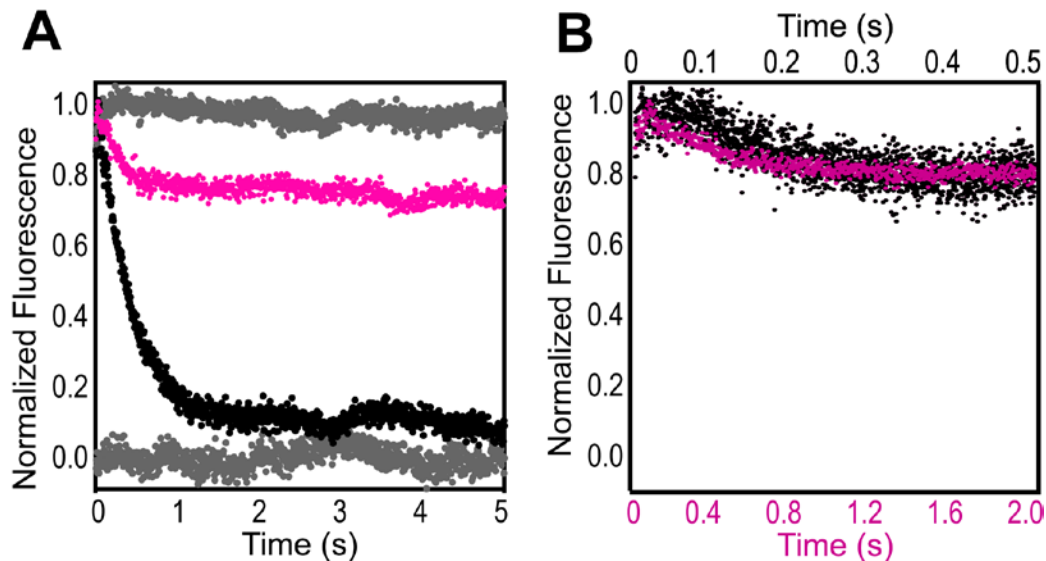
Figure 2.1. IκBα 5×PEST does not mediate the dissociation of NFκB from DNA.
(A) SFF traces corresponding to the dissociation of DNA^P (0.12 μM) from NFκB (0.1 μM) in the presence of a five-fold excess IκBα WT (●) and a five-fold excess IκBα 5×PEST (●). For reference, traces of NFκB-DNA^P and DNA^P injected against buffer are shown at 1 and 0, respectively (●). (B) SFF traces corresponding to the injection of the NFκB-DNA complex (0.1 μM:0.12 μM) against a 5-fold (●) or 20-fold (●) excess of IκBα 5×PEST; the amplitude of the curves is not effected by the concentration of IκBα 5×PEST.

The individual IκBα PEST mutants (i.e., E282Q, E284Q, D285N, E286Q, and E287Q), each stripped NFκB from DNA^P at rates and amplitudes comparable to IκBα WT (Figure 2.2A), suggesting that the collective mutation of the acidic PEST residues was sufficient to abrogate stripping.

To ensure that the IκBα PEST mutations did not adversely affect the binding of IκBα to NFκB, we measured the binding affinity of these mutants (i.e., IκBα 5×PEST, E282Q, E284Q, D285N, E286Q, and E287Q) to NFκB by means of SFF (Figure 2.2B). Furthermore, to ensure that the IκBα PEST mutations did not affect the association rate of IκBα to the NFκB-DNA complex, we measured the association of

the IκBα PEST mutants to the NFκB-DNA complex by means of SFF (Figure 2.2C). Each of the individual IκBα PEST mutants exhibited binding affinities to NFκB and the NFκB-DNA complex similar to IκBα WT. IκBα 5×PEST bound to NFκB-DNA with affinity similar to IκBα WT, and while the binding affinity of the IκBα 5×PEST mutant to the dimerization domains of NFκB was approximately four-fold weaker than that of IκBα WT as measured by SPR ($K_D = 1.5 \times 10^{-9}$ M, 3.75×10^{-10} M, respectively) (Figure 2.2D), it still exhibited the strong binding affinity associated with the NFκB-IκBα complex.
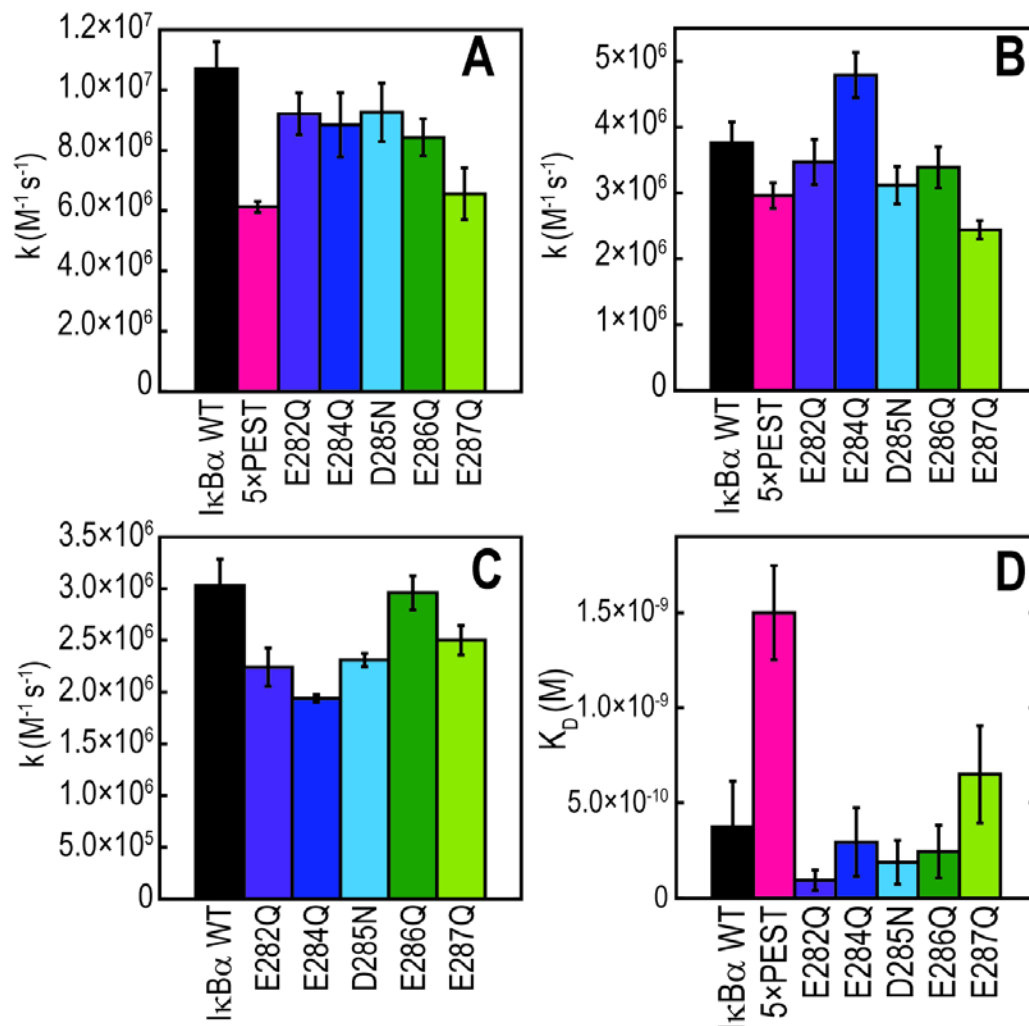
Figure 2.2. Kinetic rates of IκBα PEST mutants binding to NFκB or NFκB-DNA.
Rates of IκBα PEST mutants associating to (A) NFκB or (B) the NFκB-DNA complex as monitored by the native IκBα W258, (C) mediating the dissociation of NFκB from DNA^{P}, and (D) binding to dimerization domain NFκB.

To more deeply understand the nature of the apparent complex between NFκB, DNA^{P}, and the IκBα 5×PEST mutant observed in the SFF stripping experiment, we turned to steady-state fluorescence anisotropy, in which there is a correlation between the apparent size of a fluorescent probe and its fluorescence anisotropy signal. The aforementioned IFNκB DNA hairpin oligo was fluorescently-labeled with fluorescein

isothiocyanate to make the NFκB-DNA^F complex. When IκBα WT was added to NFκB-DNA^F at final concentrations below that of NFκB, the equilibrium fluorescence anisotropy signal remained unchanged (Figure 2.3). However, at equimolar concentrations of IκBα WT and NFκB, the equilibrium fluorescence anisotropy decreased sharply with IκBα concentration, consistent with a shift in equilibrium toward free DNA^F and formation of the highly stable NFκB-IκBα WT complex. The fluorescence anisotropy signal was not restored to that of free DNA^F (i.e., a small amount DNA^F remained bound to NFκB-IκBα WT), which is consistent with previous studies showing that NFκB-IκBα WT complex can weakly bind DNA.[2, 3]

In contrast, at equimolar concentrations of IκBα 5×PEST and NFκB, the fluorescence anisotropy signal remained higher than that of IκBα WT, signifying a greater apparent size of the fluorescently labeled DNA and suggesting the formation of a NFκB-DNA^P-IκBα 5×PEST ternary complex (Figure 2.3). Conversely, if the DNA were bound stably to the NFκB-IκBα 5×PEST complex, the fluorescence anisotropy should have increased further; instead, the signal was intermediate between that expected for free DNA^F and that of NFκB-DNA^F. The fact that the fluorescence anisotropy signal of the NFκB-DNA-IκBα 5×PEST state was lower than expected of the NFκB-DNA^F-IκBα 5×PEST ternary complex but greater than that of the NFκB-DNA-IκBα WT state suggested that either (1) the apparent size of the fluorescent probe to NFκB shifted upon IκBα 5×PEST binding (e.g., the DNA^F remained bound but in a slightly different conformation), resulting in a decreased fluorescence anisotropy signal, or (2) that DNA^F was binding to and unbinding from the NFκB-

IκBα 5×PEST complex according to the following equation: $\text{NF}\kappa\text{B-DNA}^{F}\text{-I}\kappa\text{B}\alpha$ 5xPEST $\rightleftharpoons$ $\text{NF}\kappa\text{B-I}\kappa\text{B}\alpha$ 5×PEST + DNA^{F}.
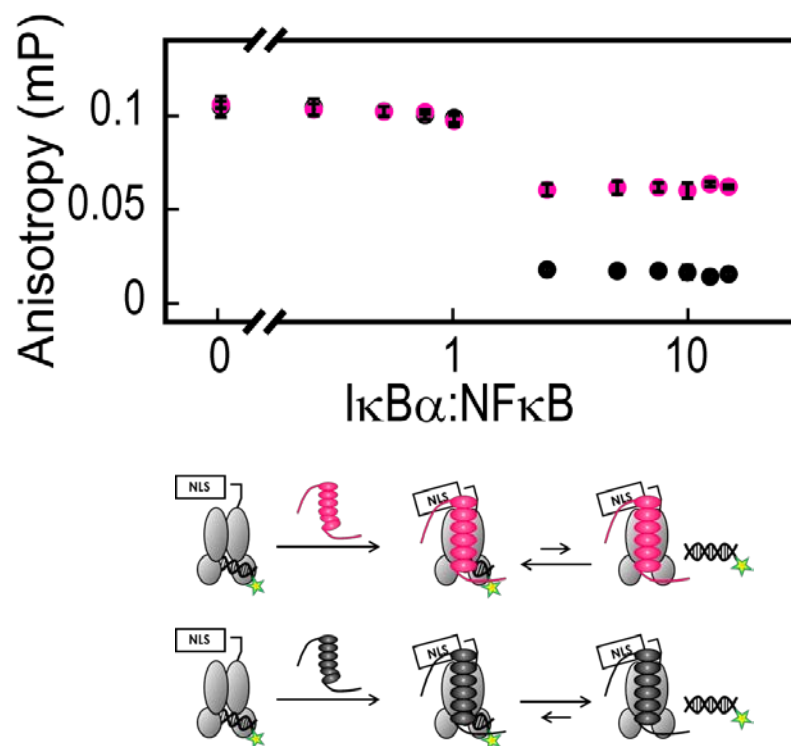
Figure 2.3. **Fluorescence anisotropy experiments suggest the formation of a stabilized ternary NFκB-DNA-IκBα 5×PEST complex.** Fluorescence anisotropy of DNA^{F} in complex with NFκB as IκBα WT (●) and IκBα 5×PEST (●) were titrated into the NFκB-DNA complex. The fluorescence anisotropy signal of free DNA^{F} was subtracted from all other signals.

To investigate whether the DNA^{F} was binding to and unbinding from the NFκB-IκBα 5×PEST complex, we used SFF to inject a 50-fold excess of unlabeled DNA against the $\text{NF}\kappa\text{B-DNA}^{P}\text{-I}\kappa\text{B}\alpha$ 5×PEST complex (Figure 2.4). As the DNA^{P} transiently exited the NFκB-IκBα 5×PEST complex, the unlabeled DNA, which was in a 50-fold excess, bound to the NFκB-IκBα 5×PEST complex, resulting in a decreased fluorescence signal over time. This experiment allows the determination of

the binding dissociation rate constant (k_d) for DNA dissociating from the NFκB-DNA^P-IκBα 5×PEST ternary complex, and the k_d was determined to be 1.67 s^{-1}, approximately three-fold faster than the rate of dissociation of DNA from NFκB (0.5 s^{-1}). These data strongly suggest that the intermediate fluorescence anisotropy signal is due to the binding and unbinding of the fluorescently-labeled DNA to the NFκB-IκBα 5×PEST complex, and the fluorescence anisotropy signal is the average of the free DNA^F signal (zero) and the NFκB-DNA-IκBα 5×PEST signal, near that observed for the NFκB-DNA complex.
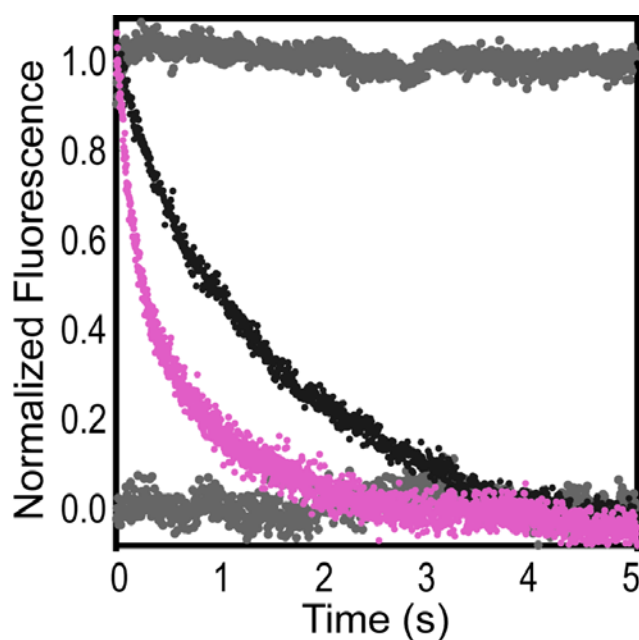
Figure 2.4. **SFF data show that DNA associates to and dissociates from the NFκB-IκBα 5×PEST complex.** Traces correspond to the transient dissociation of DNA^P from (●) the NFκB-DNA^P complex (0.61 ± 0.003 s^{-1}) and (●) NFκB-DNA^P:IκBα 5×PEST (1.67 ± 0.015 s^{-1}) in the presence of a 50-fold excess of unlabeled DNA.

Structural changes in IκBα AR5 and AR6 upon NFκB-DNA-IκBα 5×PEST ternary complex formation

Chemical shift values are sensitive to the environment around a nucleus, and chemical shift perturbation analysis is often used to discover structural changes. To further analyze the NFκB-DNA-IκBα 5×PEST ternary complex, we compared the 800 MHz HSQC-TROSY spectrum of the binary NFκB-^{2}H^{15}N IκBα 5×PEST complex with the spectrum of the ternary NFκB-DNA-^{2}H^{15}N IκBα 5×PEST complex taken under identical conditions (Figure 2.5A). The chemical shift perturbation cut-off was defined by the sum of the mean of chemical shift perturbations of all residues and one standard deviation from the mean. Comparisons between the binary NFκB-^{2}H^{15}N IκBα 5×PEST complex and the ternary NFκB-DNA-^{2}H^{15}N IκBα 5×PEST complex showed significant amide chemical shift perturbations in the following residues: Q165 (AR3), T219 (AR4), R245 (AR5), R246 (AR5), L256 (AR6), L257 (AR6), Q266 (AR6), and E284Q (PEST) (Figure 2.5B).
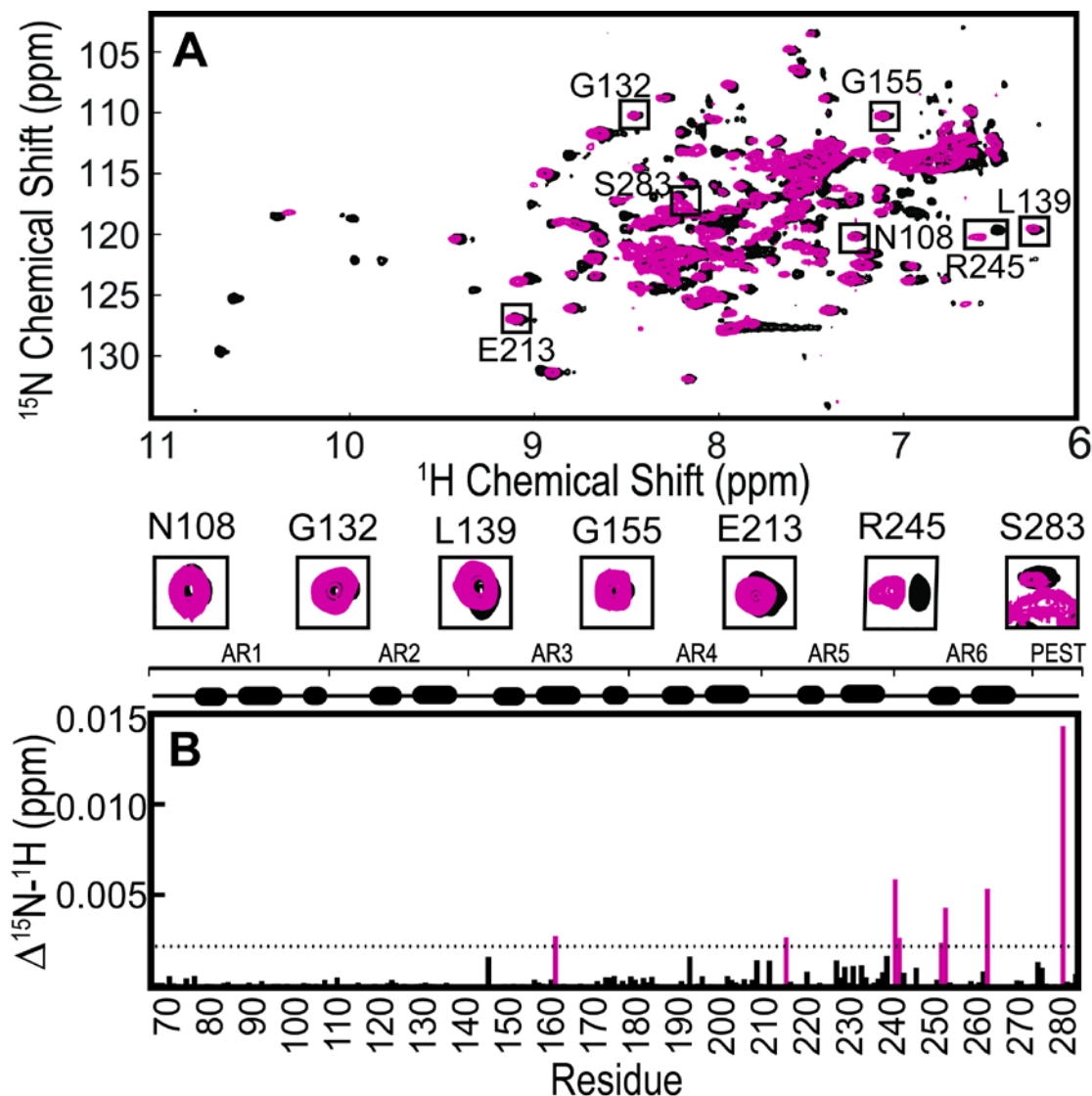
Figure 2.5. Chemical shift perturbations comparing the binary NFκB-IκBα 5×PEST complex and the ternary NFκB-DNA-IκBα 5×PEST complex. (A) Overlaid HSQC-TROSY spectra of the binary ^{2}H^{15}N IκBα 5×PEST-NFκB complex (black lines) and the ternary ^{2}H^{15}N IκBα 5×PEST:NFκB-DNA complex (pink lines) in which peaks representative of each ankyrin repeat are outlined and enlarged below. (B) Chemical shift perturbations as a function of residue number as calculated by the following equation: $([(\Delta\delta HN)^2 + (\Delta\delta NH)^2/25]/2)^{1/2}$. The dashed line reflects a cutoff of one standard deviation from the mean chemical shift perturbation of all residues. Residues exceeding this cut-off are indicated with pink bars and include Q165 (AR3), T219 (AR4), R245 (AR5), R246 (AR5), L256 (AR6), L257 (AR6), Q266 (AR6), and E284Q (PEST).

The binary NFκB-IκBα and ternary NFκB-DNA-IκBα complexes of both IκBα WT and IκBα 5×PEST were also analyzed by HDXMS to investigate differences in amide exchange in IκBα between the binary and ternary complexes; IκBα AR3, AR5/AR6, and the PEST sequence showed interesting deuterium uptake trends.

When compared to the binary NFκB-IκBα WT and NFκB-IκBα 5×PEST complexes and the ternary NFκB-DNA-IκBα WT complex, the presence of DNA in the NFκB-DNA-IκBα 5×PEST complex resulted in increased amide deuteron incorporation in the five IκBα 5×PEST peptides spanning residues 158-176, 202-234, and 237-274, which comprise AR3, AR5, and AR6—the same regions of IκBα 5×PEST that showed chemical shift perturbations due to DNA binding in the HSQC-TROSY experiments (Figure 2.6I, L-P).

The PEST sequences of both IκBα WT and IκBα 5×PEST did not exhibit significant changes in amide deuterium incorporation with DNA addition to the NFκB-IκBα complex, as evidenced in the peptide of mass 1562.65/1557.73 (IκBα WT/5×PEST 275-287) (Figure 2.6R). However, the PEST sequence of the IκBα 5×PEST mutant in the NFκB-complex exhibited increased amide exchange when compared to the NFκB-IκBα WT complex, as exhibited in the PEST sequence peptide of mass 1562.65/1557.73 (IκBα WT/5×PEST residues 275-287). This trend is consistent with the previous observation that the acidic PEST residues of IκBα WT contact Arg residues in the NFκB DNA-binding domain;[13] the IκBα 5×PEST mutant, which would not be able to make these electrostatic contacts, exhibited higher amide exchange in this region.
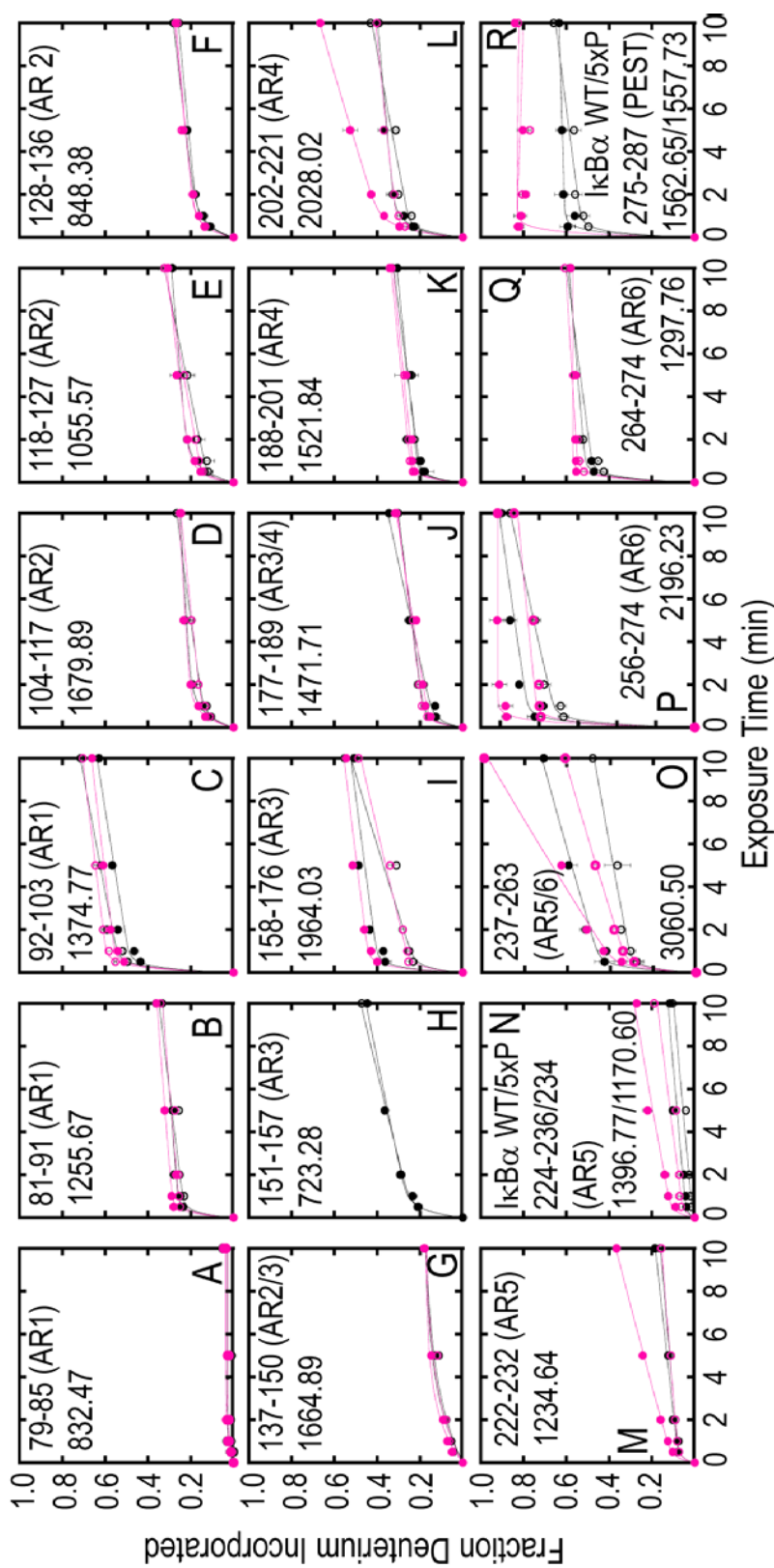
Figure 2.6. Amide H/D exchange plots of IκBα peptides comparing the NFκB-IκBα WT complex (●), the NFκB-DNA-IκBα WT complex (○), the NFκB-IκBα 5×PEST complex (○), and the NFκB-DNA-IκBα 5×PEST complex (●). (I) The IκBα peptide 158-176 of AR3 showed increased exchange in both NFκB-DNA-IκBα WT and NFκB-DNA-IκBα 5×PEST compared to NFκB-IκBα WT and NFκB-IκBα 5×PEST. (L-P) IκBα peptides from AR5 and AR6 showed increased exchange in NFκB-DNA-IκBα 5×PEST when compared to NFκB-DNA-IκBα WT, NFκB-IκBα 5×PEST, and NFκB-DNA-IκBα WT. (R) The IκBα peptide from the PEST sequence shows increased exchange in IκBα 5×PEST when compared to IκBα WT; however, the presence of DNA does not significantly affect amide exchange in either IκBα WT or IκBα 5×PEST.

Discussion

Previous stopped-flow kinetic experiments revealed formation of a very transient ternary complex during the IκBα-mediated dissociation of NFκB from DNA. Because the binding affinity of IκBα for NFκB is so much tighter (40 pM)[5] than the binding affinity of DNA for NFκB (3 nM),[2] once IκBα associates with the NFκB-DNA complex, "molecular stripping" occurs, wherein the DNA binding affinity is weakened and the highly stable NFκB-IκBα complex forms. We surmised that electrostatic repulsion between the DNA and the IκBα PEST sequence would play an important role in the weakened DNA binding, and indeed results presented here demonstrate that neutralization of the PESEDEE sequence to PQSQNQQ allows formation of a more stable ternary complex between NFκB, DNA, and IκBα.

SFF-monitored association of the IκBα 5×PEST mutant to the NFκB-DNA complex did not show the dramatic decrease in fluorescence of the NFκB-bound pyrene-labeled DNA that was observed upon association of IκBα WT, indicative of dissociation of the labeled DNA. Instead, a stable signal higher than that of free DNA[P] persisted as if the DNA were still bound to the NFκB-IκBα 5×PEST in a ternary complex. Stead-state fluorescence anisotropy studies corroborated these findings but suggested that DNA was still rapidly associating and dissociating from the ternary complex; this was also confirmed by DNA dissociation measurements again using SFF.

Even though the DNA was rapidly associating and dissociating, the affinity of the DNA for the NFκB-IκBα 5xPEST complex was clearly stronger than for the

NFκB-IκBα WT complex. The electrostatic repulsion also apparently involves competition for interaction with the same positively charged Arg residues in the NFκB DNA-binding domain. HDXMS results show that the neutralized IκBα 5×PEST mutant has higher amide exchange in the PEST region than does the WT PEST sequence. This result is striking because the PEST sequence is highly disordered and expected to undergo rapid amide exchange, but in the WT IκBα, it does not exchange as rapidly as in the 5×PEST mutant. Based on previous NMR evidence,[13] it is most likely that the negatively charged WT PEST sequence has lower exchange because of electrostatic interactions with positively charged Arg residues in the DNA-binding domain of NFκB—an interaction that is eliminated in the IκBα 5×PEST mutant.

Even though introduction of the 5×PEST mutation in IκBα stabilized the ternary complex, the DNA was still not very stably bound. We therefore turned to experimental methods that could give information about the structure of the ternary complex in solution where a slight excess of DNA would shift the equilibrium to predominantly the ternary complex. The question we were most interested in addressing was whether or not the AR domain of IκBα was fully folded and bound. We had previously shown that AR5 and AR6 of IκBα fold upon binding to NFκB,[14] but it was not clear whether this coupled folding and binding would occur while DNA was still bound. It was possible that only the PEST sequence needed to move to accommodate the DNA, but it was also possible that the coupled folding and binding of the IκBα AR domain would not be completed in the presence of DNA. The NMR and HDXMS data strongly suggest that ternary complex formation, which is stabilized in the IκBα 5×PEST mutant ternary complex, involves structural "accommodation" of

the DNA by the IκBα AR domain. The accommodation appears to involve regions of the AR domain that are far from the DNA, including AR3, as well as AR5 and AR6. The dramatic differences in chemical shifts as well as the overall increased amide exchange in parts of AR3, as well as all of AR5 and AR6 are most consistent with a structure in which the coupled folding and binding of the IκBα ARD has only partly occurred when DNA is still bound. It is interesting to speculate, therefore, that part of the driving force for the IκBα-mediated "molecular stripping" of NFκB from DNA is the electrostatic repulsion of the DNA by the IκBα PEST sequence, but it appears to also be driven by the folding and binding of IκBα AR5 and AR6 to NFκB.

Acknowledgements

References

1. Bergqvist, S., Alverdi, V., Mengel, B., Hoffmann, A., Ghosh, G., and Komives, E. A. (2009) Kinetic enhancement of NF-kappaB•DNA dissociation by IkappaBalpha, *Proc. Nat. Acad. Sci. U.S.A. 106*, 19328-19333.

2. Alverdi, V., Hetrick, B., Joseph, S., and Komives, E. A. (2014) Direct observation of a transient ternary complex during IkBa-mediated dissociation of NFkB from DNA, *Proc Natl Acad Sci U S A 111*, 225-230.

3.   Sue, S. C., Alverdi, V., Komives, E. A., and Dyson, H. J. (2010) Detection of a ternary complex of NFkB and IkBa with DNA provides insight into how IkBa removes NFkB from transcription sites, *Proc Natl Acad Sci U S A 108*, 1367-1372.

4.   Bergqvist, S., Ghosh, G., and Komives, E. A. (2008) The IkBa/NF-kB complex has two hot-spots, one at either end of the interface, *Prot. Sci. 17*, 2051-2058.

5.   Bergqvist, S., Croy, C. H., Kjaergaard, M., Huxford, T., Ghosh, G., and Komives, E. A. (2006) Thermodynamics reveal that helix four in the NLS of NF-kappaB p65 anchors IkappaBalpha, forming a very stable complex, *J. Mol. Biol. 360*, 421-434.

6.   Croy, C. H., Bergqvist, S., Huxford, T., Ghosh, G., and Komives, E. A. (2004) Biophysical characterization of the free IkappaBalpha ankyrin repeat domain in solution, *Protein Sci 13*, 1767-1777.

7.   Cervantes, C. F., Markwick, P. R. L., Sue, S. C., McCammon, J. A., Dyson, H. J., and Komives, E. A. (2009) Functional dynamics of the folded ankyrin repeats of IkappaB alpha revealed by nuclear magnetic resonance. , *Biochemistry 48*, 8023-8031.

8.   Sue, S. C., Cervantes, C., Komives, E. A., and Dyson, H. J. (2008) Transfer of Flexibility between Ankyrin Repeats in IkappaBalpha upon Formation of the NF-kappaB Complex., *J. Mol. Biol. 380*, 917-931.

9.   Dembinski, H., Wismer, K., Balasubramaniam, D., Gonzalez, H. A., Alverdi, V., Iakoucheva, L., and Komives, E. A. (2014) Predicted disorder-to-order transition mutations in IkBa disrupt function, *Physical Chemistry Chemical Physics 16*, 6480-6485.

10.   Struder, S. M., and Joseph, S. (2007) Binding of mRNA to the Bacterial Translation Initiation Complex, *Methods in Enzymology 430*, 31-44.

11.   Mulvihill, M., Guttman, M., and Komives, E. A. (2011) Protein interactions among F65, the low-density lipoprotein receptor-related protein, and the amyloid precursor protein, *Biochemistry-Us 50*, 6208-6216.

12.   Wales, T. E., Fadgen, K. E., Gerhardt, G. C., and Engen, J. R. (2008) High-speed and high-resolution UPLC separation at zero degrees Celsius, *Anal. Chem. 80*, 6815–6820.

13.   Sue, S. C., and Dyson, H. J. (2009) Interaction of the IkappaBalpha C-terminal PEST sequence with NF-kappaB: insights into the inhibition of NF-kappaB DNA binding by IkappaBalpha., *J Mol Biol. 388*, 824-838.

14.   Truhlar, S. M. E., Mathes, E., Cervantes, C. F., Ghosh, G., and Komives, E. A. (2008) Pre-folding IkappaBalpha alters control of NF-kappaB signaling., *J. Mol. Biol. 380*, 67 - 82.

Chapter 3

Probing the Role of IκBα-mediated NFκB Dissociation from DNA in Mouse Embryonic Fibroblasts

Introduction

As mentioned in Chapter 2, six years ago our lab first described SPR experiments revealing that IκBα dramatically increased the rate of dissociation of NFκB from target DNA.[1] Even with this initial report, questions were immediately raised as to whether the phenomenon was relevant inside the nucleus and which genes might require such rapid removal of NFκB from the promoter sequence. To begin to answer that question, our lab pursued a collaboration with the Hoffmann Lab, now at the University of California, Los Angeles.

First, it was necessary to find a mutation in IκBα that would render it significantly less able to "strip" NFκB from its target DNA without compromising its capacity to bind to NFκB. Initial hopes were placed on the Y254L/T257A double mutant of IκBα, which was shown to strip NFκB from DNA less efficiently, but its 10-fold weaker binding affinity for NFκB rendered the system leaky inside cells, and a significant portion of NFκB was found in the nucleus even in resting cells.[2] As described in Chapter 2, the discovery of the IκBα 5×PEST mutant, which is apparently less efficient at promoting NFκB dissociation from DNA, reinvigorated hopes of demonstrating the intracellular consequences of impaired stripping. While the *in vitro* studies presented in Chapter 2 were performed with the minimal fragment of IκBα (residues 67-287), in this chapter, the studies are extended to full-length IκBα (residues 1-317). First, work designed to explore the *in vitro* functional consequences of the 5×PEST mutations in IκBα$_{(1-317)}$ is presented. After this, some encouraging preliminary results from the Hoffmann Lab are presented in which the 5×PEST

mutations were introduced into IκBα$_{(1-317)}$ in an expression system under control of the naturally occurring promoter. The results suggest that in fact, the 5×PEST mutations increase the nuclear residence time of the mutant IκBα consistent with an impaired stripping function.

Materials and Methods

Protein expression and purification

Human wild-type N-terminal hexahistidine-IκBα$_{(1-317)}$, the human N-terminal hexahistidine-IκBα$_{(1-317)}$ 5×PEST mutant, and murine, N-terminal hexahistidine-p50$_{39–350}$/RelA$_{19–321}$ heterodimer (NFκB) were expressed as described previously[3, 4] and purified by nickel affinity chromatography (Ni-NTA Agarose, Qiagen, Valencia, CA, USA). NFκB was then purified by cation exchange chromatography (Mono S column, GE Healthcare). Proteins were then purified by size exclusion chromatography (Superdex 200, GE Healthcare).

Hereafter referred to as p50dd/biotin-p65dd, murine dimerization domain RelA$_{190-321}$ with an N-terminal Cys and dimerization domain p50$_{248-350}$ were expressed, purified, and prepared for surface plasmon resonance as described.[4, 5]

Protein concentrations were determined by spectrophotometry at 280 nm (NFκB ε = 43760 M^{-1} cm^{-1}, IκBα WT and IκBα 5×PEST ε = 28420 M^{-1} cm^{-1}). Unless otherwise noted, experiments were performed with proteins in 25 mM Tris pH 7.5, 150 mM NaCl, 1 mM DTT, 0.5 mM EDTA.

DNA labeling and purification

A hairpin DNA sequence corresponding to the IFN-κB site 5'-AmMC6/GGGAAATTCCTCCCCCAGGAATTTCCC-3' (IDT Technologies, Coranville, CT, USA) was labeled with pyrene (N-hydroxyl succinimide ester) (DNA^P) or fluorescein (fluorescein isothiocyanate) (DNA^F) as described.[6]

Stopped-flow fluorescence

Stopped-flow fluorescence (SFF) experiments were performed on an SX-20 stop-flow apparatus (Applied Photophysics, Leatherhead, UK) at 25 °C set to collect 2000 pt linearly with a final mixing volume of 200 µL. The IκBα-mediated dissociation of DNA^P from NFκB was monitored by adding different concentrations of IκBα WT (0.25, 0.50, 0.75, 1.00, 1.25, 1.50, 1.75, and 2.00 µM) to a 1.00 µM NFκB-1.20 µM DNA^P complex monitoring the change in fluorescence of the pyrene-labeled DNA. The pyrene was excited at 343 nm, and the fluorescence emission was monitored at 376 nm with a cut-off filter at 350 nm. The association of IκBα to NFκB or NFκB-DNA was monitored via the native Trp fluorescence of a single Trp at position 258 in IκBα by exciting at 280 nm and monitoring the emission at 345-355 nm with a cut-off filter at 320 nm. Various concentrations of NFκB or NFκB-DNA (0.30, 0.40, 0.50, 0.60, 0.70, 0.80 µM) were mixed with IκBα (0.10 µM). Data were collected and analyzed as described.[5]

Surface Plasmon resonance experiments

Sensorgrams were recorded on a Biacore 3000 instrument using streptavidin chips (GE Healthcare) by immobilizing 150, 250, 350 RU of p50dd/biotin-p65dd on flow cells 2, 3, and 4, respectively, leaving flow cell 1 unmodified for reference subtraction. NFκB binding experiments were conducted on IκBα WT, E282Q, E284Q, D285N, E286Q, E287Q, and 5×PEST, and the data were analyzed as described.[5, 7]

Fluorescence anisotropy

Fluorescence anisotropy data were collected in triplicate on a Beckman Coulter DTX 880 Multimode Detector by exciting fluorescein-labeled DNA at 495 nm and monitoring emission at 519 nm. DNA^F (10 nM) and NFκB (200 nM) were incubated overnight. The NFκB-DNA complex (100 µL) was added to 100 µL IκBα WT or IκBα 5x PEST at final IκBα concentrations of 0, 10, 25, 50, 75, 100, 250, 500, 750, 1000, 1250, and 1500 nM and incubated 1 h at 25 °C prior to data collection. Anisotropy values were calculated according to the equation $r = [I_{(V,V)} - GI_{(V,H)}]/[I_{(V,V)} - 2GI_{(V,H)}]$, where r is anisotropy, $I_{(V,V)}$ is the fluorescence intensity in the parallel direction, $I_{(V,H)}$ is the fluorescence intensity in the perpendicular direction, and G is 0.67, a correction factor for the difference in detection sensitivity for parallel and perpendicular polarized light.[8] Fluorescence anisotropy values reported here were corrected for the anisotropy signal due to free DNA^F.

DNA constructs for intracellular experiments

NFκB-inducible IκBα constructs were derived from an MFG-derived self-inactivating retrovirus backbone (HRSpuro) modified to express the IκBα transgene under the control of five tandem kB sites upstream of a minimal promoter. IκBα mutant forms were produced using site-directed mutagenesis. For live-cell studies, AcGFP1 was fused to the N-terminus of RelA and the resulting construct was sub-cloned into the constitutively expressing retroviral plasmid pBabe-Hygro.

Mouse embryonic fibroblast transfection

Cells were transfected together with pCL.Eco into 293T cells with Lipofectamine 2000 transfection reagent (Invitrogen) for 48 h. Supernatant was filtered and used to infect MEFs. Transduced cells were selected with puromycin hydrochloride (Sigma). Cells were plated onto 35 mm glass bottom dishes (MatTek) or iBidi 8 well chambers (iBidi) 24 h prior to stimulation and immediate imaging.

Microscopic Imaging

Images were acquired on an Axio Observer Z1 inverted microscope (Carl Zeiss Microscopy GmbH, Germany) with a 40x, 1.3 NA oil-immersion, or 20x, 0.8 NA air-immersion objective to a Coolsnap HQ2 CCD camera (Photometrics, Canada) using ZEN imaging software (Carl Zeiss Microscopy GmbH, Germany). Environmental conditions were maintained in a humidified chamber at 37º C, 5% CO_2 (Pecon, Germany). Quantitative image processing was performed using the FIJI distribution of

Image J (NIH). All cells of each frame in the microscope imaging experiments were measured for total fluorescence intensity. Time course data were normalized by the minimum and maximum values to account for the varying overall intensities of different cells. The single cell traces were averaged and error bars in the mean curves are the standard deviation from the mean.

Results

IκBα$_{(1-317)}$ 5×PEST mutant forms a ternary NFκB-DNA-IκBα complex

We compared the IκBα-mediated stripping of NFκB from DNA by SFF using IκBα$_{(1-317)}$ WT and the IκBα$_{(1-317)}$ 5×PEST mutant (Figure 3.1). It has been demonstrated that a pyrene-labeled IFNκB hairpin DNA oligo exhibits increased fluorescence upon binding to NFκB, and when IκBα strips NFκB from DNA^P, a decrease in fluorescence signal is observed.[1] IκBα$_{(1-317)}$ WT stripped NFκB from DNA^P, restoring the fluorescence signal to that of free DNA^P; however, the IκBα$_{(1-317)}$ 5×PEST mutant did not strip NFκB from DNA^P to the fluorescence signal of free DNA^P, suggesting that some of the DNA^P remained bound. If the stripping capacity of the IκBα$_{(1-317)}$ 5×PEST mutant were diminished but not abolished, adding an excess of IκBα$_{(1-317)}$ 5×PEST to the stripping reaction would result in decreased fluorescence signal, reflective of free DNA^P; however, when we added a twenty-fold excess of IκBα$_{(1-317)}$ 5×PEST, the rate of the reaction increased, but the change in amplitude in

the SFF trace remained constant (Figure 3.1B). These data suggest that the IκBα$_{(1-317)}$

5×PEST mutant did not strip NFκB from DNA^P and that the DNA^P remained bound.
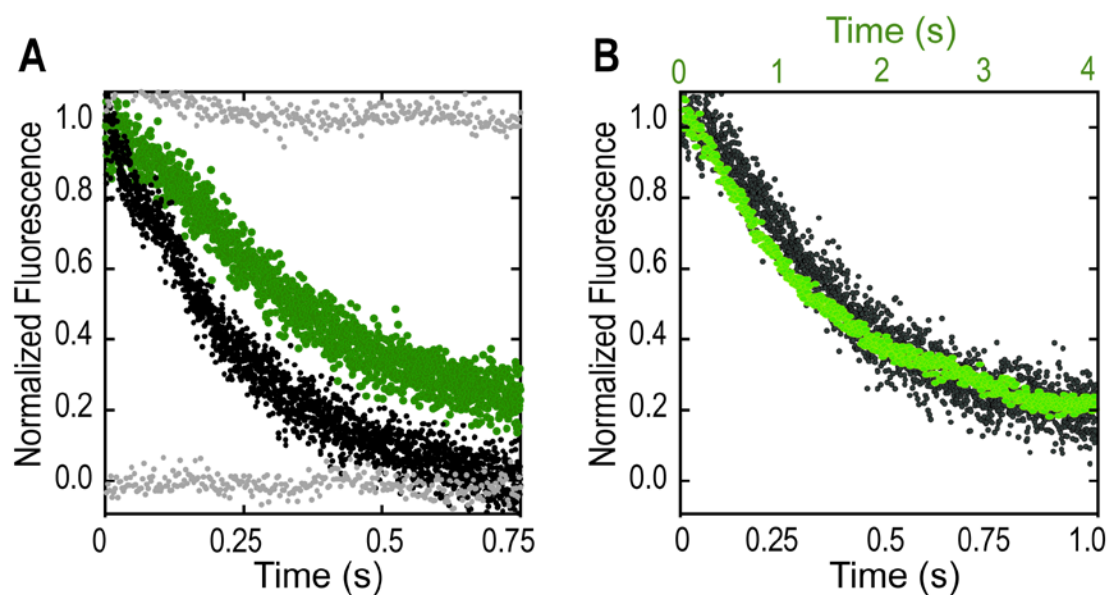
Figure 3.1. IκBα$_{(1-317)}$ 5×PEST does not mediate the dissociation of NFκB from DNA. SFF traces corresponding to the dissociation DNA^P (0.12 μM) from NFκB (0.1 μM) in the presence of a five-fold excess IκBα$_{(1-317)}$ WT (●) and a five-fold excess IκBα$_{(1-317)}$ 5×PEST (●). For reference, traces of NFκB-DNA^P and DNA^P injected against buffer are shown at 1 and 0, respectively (●). (B) SFF traces corresponding to the injection of the NFκB-DNA complex (0.1 μM:0.12 μM) against a 5-fold (●) or 20-fold (●) excess of IκBα 5×PEST; the amplitude of the curves is not effected by the concentration of IκBα 5×PEST.

To ensure that the IκBα$_{(1-317)}$ 5×PEST mutations did not adversely affect the

binding to NFκB, we measured its binding affinity to NFκB by means of SFF (Figure

3.2A); the association of IκBα$_{(1-317)}$ 5×PEST [1.52 (±0.002) × 10^5 M^{-1}s^{-1}] was

approximately two-fold slower than that of IκBα$_{(1-317)}$ WT [3.65 (±0.003) × 10^5 M^{-1}s^{-1}

]. Furthermore, to ensure that the IκBα$_{(1-317)}$ 5×PEST mutation did not affect the

association rate to the NFκB-DNA complex, we measured the association of the

IκBα$_{(1-317)}$ 5×PEST mutant NFκB-DNA complex by means of SFF (Figure 3.2B).

IκBα$_{(1-317)}$ 5×PEST bound to the NFκB-DNA complex with affinity similar to IκBα$_{(1-317)}$ WT [IκBα WT = 3.33 (±0.03) × 10^5 M^{-1}s^{-1}; IκBα 5×PEST = 2.58 (±0.02) × 10^5 M^{-1}s^{-1}].
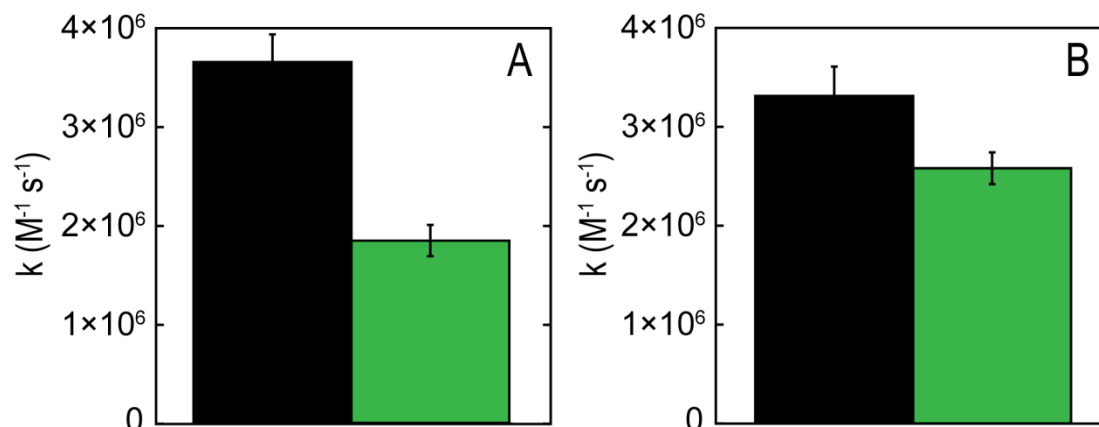
Figure 3.2. Kinetic rates of IκBα$_{(1-317)}$ WT (black) and IκBα$_{(1-317)}$ 5×PEST (green) associating to (A) NFκB or (B) the NFκB-DNA complex as monitored by the native IκBα W285.

The NFκB binding affinity of IκBα$_{(1-317)}$ 5×PEST was compared to that of IκBα$_{(1-317)}$ WT by SPR. While the binding affinity of the IκBα$_{(1-317)}$ 5×PEST mutant to the dimerization domain of NFκB was approximately three-fold weaker than that of IκBα$_{(1-317)}$ WT (K$_D$ = 5.9 ×10^{-11} M, 2.1×10^{-10} M, respectively) (Figure 3.3, Table 3.1), it still exhibited the strong binding affinity associated with the NFκB-IκBα complex.
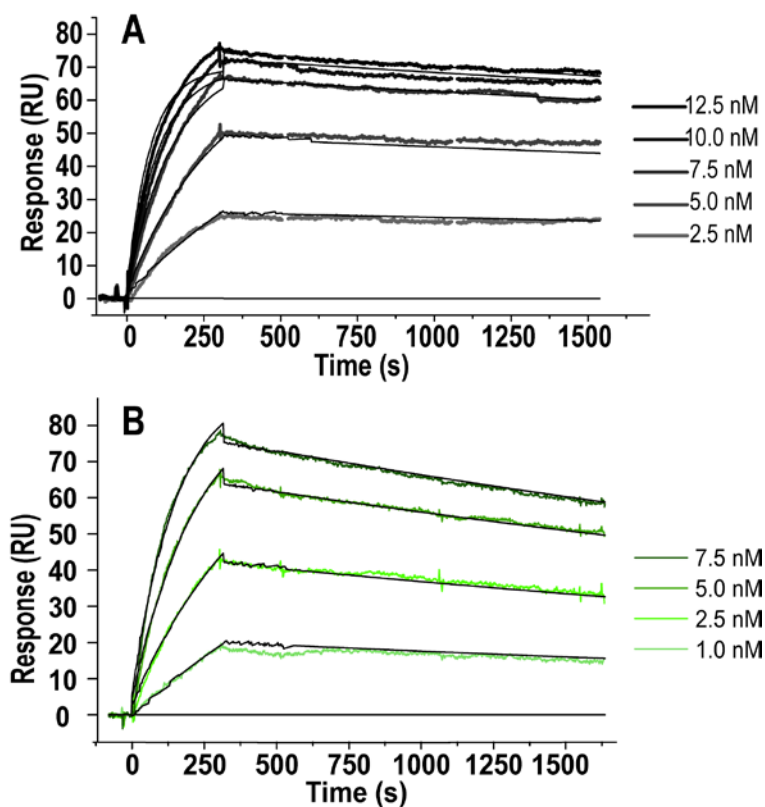
Figure 3.3. **SPR traces for the binding of (A) IκBα$_{(1\text{-}317)}$ WT and (B) the IκBα$_{(1\text{-}317)}$ 5×PEST mutant to p50dd/biotin-p65dd.** The binding constants derived from these binding curves are given in Table 3.1.

Table 3.1. Kinetic rates derived from SPR experiments of IκBα$_{(1\text{-}317)}$ WT and 5×PEST binding to p50dd/biotin-p65dd.

	k_a (M^{-1}s^{-1})		k_d (M^{-1})		K_D (M)	
	Average	Standard Deviation	Average	Standard Deviation	Average	Standard Deviation
IκBα WT	1.4E+06	3.3E+03	8.1E-05	1.3E-06	5.9E-11	4.1E-12
IκBα 5×PEST	9.3E+05	2.1E+03	1.9E-04	1.3E-06	2.1E-10	6.2E-12

To more deeply understand the nature of the apparent complex between NFκB, DNA^P, and the IκBα$_{(1-317)}$ 5×PEST mutant observed in the SFF stripping experiment, we turned to steady-state fluorescence anisotropy, in which there is a correlation between the apparent size of a fluorescent probe and its fluorescence anisotropy signal. The aforementioned IFNκB DNA hairpin oligo was fluorescently labeled with fluorescein isothiocyanate, and the NFκB-DNA^F complex was prepared. When IκBα WT was added to NFκB-DNA^F and at final concentrations below that of NFκB, the equilibrium fluorescence anisotropy signal remained unchanged (Figure 3.4). However, at equimolar concentrations of IκBα$_{(1-317)}$ WT and NFκB, the equilibrium fluorescence anisotropy decreased sharply with IκBα$_{(1-317)}$ WT concentration, consistent with a shift in equilibrium toward free DNA^F and formation of the highly stable NFκB-IκBα$_{(1-317)}$ WT complex. The fluorescence anisotropy signal was not restored to that of free DNA^F (i.e., a small amount DNA^F remained bound to NFκB-IκBα$_{(1-317)}$ WT complex), which is consistent with previous studies showing that NFκB-IκBα$_{(1-317)}$ WT complex can weakly bind DNA.[9, 10]

At equimolar concentrations of IκBα$_{(1-317)}$ 5×PEST and NFκB, the fluorescence anisotropy signal remained higher than that of IκBα$_{(1-317)}$ WT, signifying a greater apparent size of the fluorescently labeled DNA and suggesting the formation of a NFκB-DNA^P-IκBα 5×PEST ternary complex. In the case of the NFκB-IκBα$_{(1-317)}$ 5×PEST complex, the fluorescence anisotropy signal was only a little higher than for the ternary complex formed with IκBα$_{(1-317)}$ WT. Thus, the full-length IκBα$_{(1-317)}$ 5×PEST did not form as stable of a ternary complex as was observed for the IκBα$_{(67-287)}$ 5×PEST (see Chapter 2).
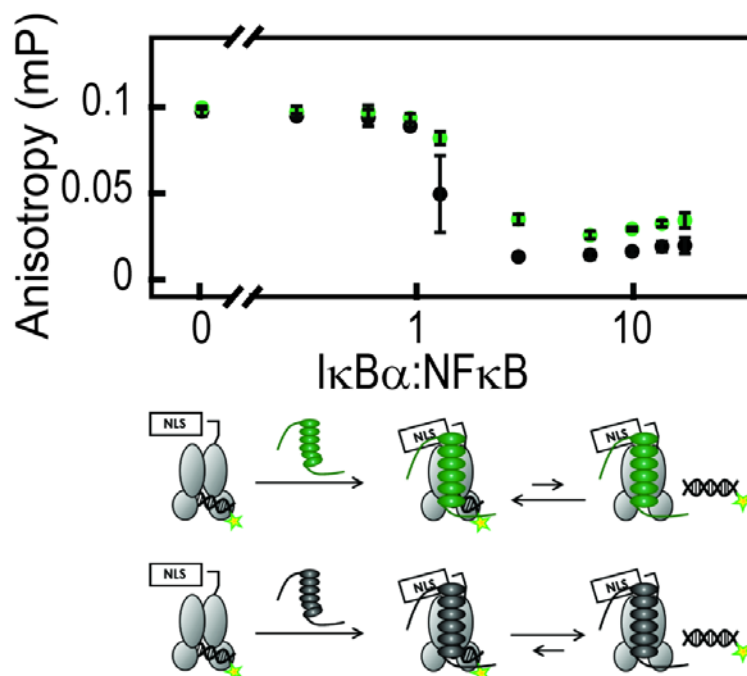
Figure 3.4. Fluorescence anisotropy experiments suggest the formation of a stabilized ternary NFκB-DNA-IκBα(1-317) complex. DNA^F in complex with NFκB as IκBα(1-317) WT (●) and IκBα(1-317) 5×PEST (●) were titrated into the NFκB-DNA complex. The fluorescence anisotropy signal of free DNA^F was subtracted from all other signals.

To measure the rate of dissociation of DNA^F from the NFκB-IκBα(1-317) 5×PEST complex, we used SFF to inject a 50-fold excess of unlabeled DNA against the NFκB-DNA^P-IκBα(1-317) 5×PEST complex (Figure 3.5). As the DNA^P transiently exited the NFκB-IκBα(1-317) 5×PEST complex, the unlabeled DNA, which was in a 50-fold excess, bound to the NFκB-IκBα(1-317) 5×PEST complex, resulting in a decreased fluorescence signal over time. These data show that the rate of dissociation of DNA from the ternary NFκB-DNA-IκBα(1-317) 5×PEST complex was 1.841 ± 0.003 s^{-1}, three-fold faster than the rate at which DNA dissociates from the NFκB-DNA complex (0.613 ± 0.003 s^{-1}).
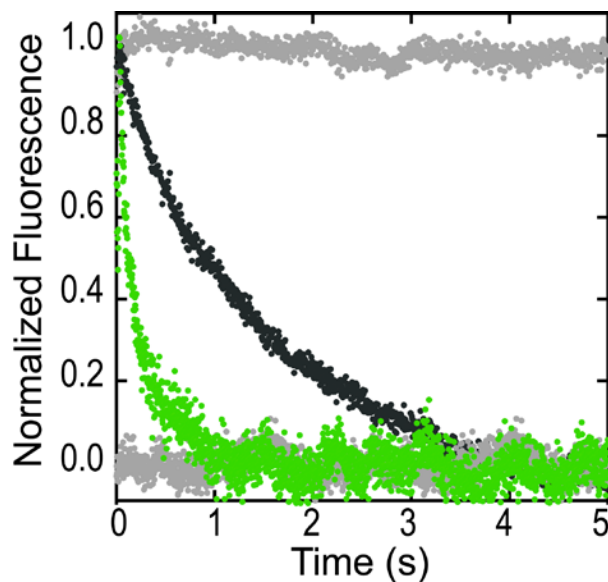
Figure 3.5. **SFF studies suggest that DNA associates to and dissociates from the NFκB-DNA-IκBα(1-317) ternary complex.** Traces corresponding to the transient dissociation of DNA^P from (●) the NFκB-DNA^P complex (0.61 ± 0.003 s^{-1}) and (●) NFκB-DNA^P:IκBα(1-317) 5×PEST (1.84 ± 0.003 s^{-1}) in the presence of a 50-fold excess of unlabeled DNA.

The IκBα(1-317) 5×PEST mutant does not export NFκB from the nucleus

To investigate the importance of NFκB regulation by IκBα, mouse embryonic fibroblast cells (MEFs) expressing GFP-NFκB were transfected with plasmids encoding either IκBα WT or IκBα 5×PEST under control of the κB promoter (Figure 3.6A). In resting cells, IκBα sequesters NFκB to the cytosol; upon stimulation, IκBα is degraded, NFκB enters the nucleus and upregulates genes downstream of the κB promoter, one of which is IκBα. Newly synthesized IκBα can then enter the nucleus and mediate the dissociation of NFκB from DNA. When the MEF transfectants were stimulated with TNFα, we observed a sudden surge of nuclear GFP-NFκB

corresponding to the degradation of IκBα and the nuclear translocation of GFP-NFκB (Figure 3.6B). The IκBα WT MEF transfectants exhibited a steep decline in nuclear NFκB at approximately 60 min, corresponding to newly synthesized IκBα WT entering the nucleus and mediating the dissociation of NFκB from DNA, resulting in the export of NFκB from the nucleus. Conversely, the IκBα 5×PEST MEF transfectants demonstrated a diminished capacity to regulate NFκB resulting in the persistence of nuclear GFP-NFκB levels.

A

Nucleus   GFP-p65   α-IκBα   Composite

B
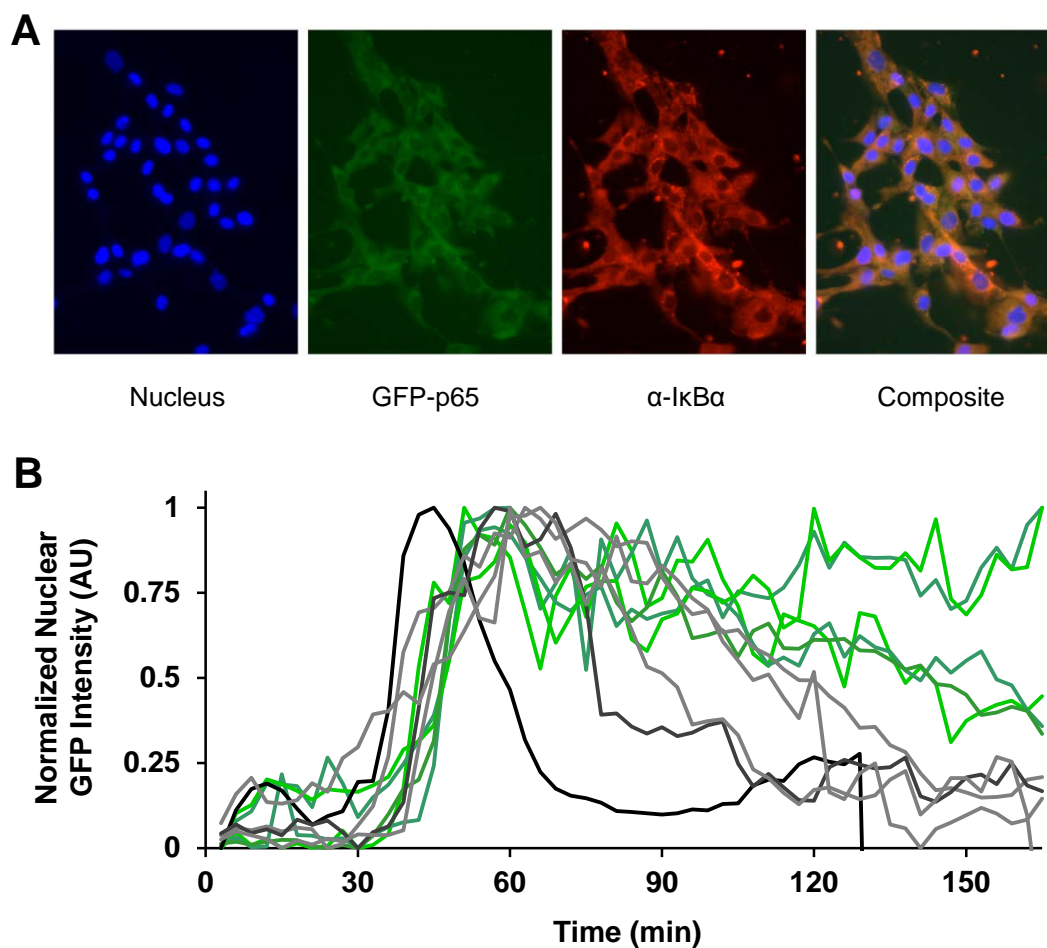
Figure 3.6. The IκBα 5×PEST mutant is deficient in regulating GFP-NFκB in live MEFs. (A) MEFs transfected with the IκBα 5×PEST plasmid with Hoechst-stained nuclei, GFP-p65, visualized with an mCherry-fused IκBα antibody, and a composite image. (B) MEF iκb$^{-/-}$ cells expressing GFP-NFκB were transfected with plasmids encoding IκBα WT (gray) or IκBα 5×PEST (green) under control of the κB promoter and were stimulated with a pulse of TNFα, and the fraction of nuclear GFP-NFκB was monitored by fluorescence microscopy. The fraction of nuclear GFP-NFκB as a function of time for five representative IκBα WT transfectants and IκBα 5×PEST transfectants are shown.

Discussion

In parallel with the $I\kappa B\alpha_{(67-287)}$ 5×PEST mutant, I have established that a stabilized ternary NFκB-DNA-IκBα complex can form when the five of the acidic IκBα PEST residues are mutated to their amide counterparts in full-length $I\kappa B\alpha_{(1-317)}$. It is interesting that the fluorescence anisotropy signal from the ternary complex formed with full-length $I\kappa B\alpha_{(1-317)}$ 5×PEST mutant does not appear to have as high of an anisotropy as that for the ternary complex formed with the $I\kappa B\alpha_{(67-287)}$ 5×PEST mutant (compare Figure 2.3 with Figure 3.4). The kinetic constants for binding of the two different IκBα's to NFκB are nearly identical, and the dissociation rate of DNA from each of the ternary complexes are also nearly identical. It is possible that in the ternary complex with the full-length $I\kappa B\alpha_{(1-317)}$ 5×PEST mutant, residues 288-317 create steric interference with the DNA re-binding. This would cause the overall equilibrium concentration of the ternary complex to be somewhat lower consistent with the observed steady state fluorescence anisotropy results.

In collaboration with the Hoffmann Lab at the University of California, Los Angeles, we have shown that the IκBα 5×PEST mutant dampens the regulation of NFκB in MEF transfectants. One pivotal implication of these data is we can now probe the importance of IκBα in NFκB regulation. It has been established that NFκB binds both to κB DNA sequences (e.g., NFκB-IgκB DNA sequence $K_D = 3$ nM) and to non-specific DNA sequences (e.g., NFκB-random DNA sequence $K_D \approx 50$ nM).[1] The fact that NFκB can bind to and unbind from specific and non-specific DNA

sequences relatively rapidly begs the following question: What is the specific role of IκBα in NFκB regulation?

One possibility is that IκBα is required to bind to regulate NFκB at promoter sequences with multiple κB binding sites; ostensibly, promoter sequences with fewer κB binding sites would bind NFκB less frequently. To explore this possibility, we plan to conduct chromatin immunoprecipitation sequencing (ChIP Seq) experiments on MEF transfectants expressing either IκBα WT or IκBα 5×PEST to probe the importance of IκBα regulation as it pertains to the number of κB binding sites in a given promoter.

Another possible role of IκBα is that it is required for nuclear export of NFκB from the nucleus. In fact, the dissociation from DNA and subsequent nuclear export may be linked since it is known that NFκB and IκBα both shuttle into and out of the nucleus. Apparently, the sequestration of the nuclear localization signal of one subunit of the NFκB dimer by the bound IκBα changes the equilibrium of shuttling to favor the cytoplasmic localization. In addition, IκBα contains a nuclear export signal that also facilitates the re-distribution of bound NFκB dimers to the cytoplasm.[11]

While these results have exciting implications, it is recognized that a more thorough investigation of the effects of the IκBα 5×PEST mutation is needed. To assess the effect of IκBα 5×PEST mutant on NFκB-DNA binding, an electrophoretic mobility shift assay will be employed; given the SFF and equilibrium fluorescence anisotropy data presented in this work, it is highly probable that the IκBα 5×PEST mutant will affect the binding affinity of NFκB to DNA.[12] To probe the effect of the mutations on IκBα degradation rates, quantitative western blots will be employed to

monitor cellular IκBα levels on either IκBα 5×PEST or IκBα WT MEF transfectants treated with cyclohexamide.[13]

Acknowledgements

Chapter 3, in full, is material in preparation for journal submission to which the dissertation author contributed equally with J. Vargas. The material will be submitted for publication (**Dembinski, H.**, Vargas, J., Peacock, R., Wismer, K., Hoffmann, A., Komives, E.A. Functional consequences of IκBα-mediated accelerated dissociation of NFκB from transcription sites).

References

1.   Bergqvist, S., Alverdi, V., Mengel, B., Hoffmann, A., Ghosh, G., and Komives, E. A. (2009) Kinetic enhancement of NF-kappaB•DNA dissociation by IkappaBalpha, *Proc. Nat. Acad. Sci. U.S.A. 106*, 19328-19333.

2.   Truhlar, S. M. E., Mathes, E., Cervantes, C. F., Ghosh, G., and Komives, E. A. (2008) Pre-folding IkappaBalpha alters control of NF-kappaB signaling., *J. Mol. Biol. 380*, 67 - 82.

3.   Sue, S. C., Cervantes, C., Komives, E. A., and Dyson, H. J. (2008) Transfer of Flexibility between Ankyrin Repeats in IkappaBalpha upon Formation of the NF-kappaB Complex., *J. Mol. Biol. 380*, 917-931.

4.   Bergqvist, S., Croy, C. H., Kjaergaard, M., Huxford, T., Ghosh, G., and Komives, E. A. (2006) Thermodynamics reveal that helix four in the NLS of NF-kappaB p65 anchors IkappaBalpha, forming a very stable complex, *J. Mol. Biol. 360*, 421-434.

5.   Dembinski, H., Wismer, K., Balasubramaniam, D., Gonzalez, H. A., Alverdi, V., Iakoucheva, L., and Komives, E. A. (2014) Predicted disorder-to-order transition mutations in IkBa disrupt function, *Physical Chemistry Chemical Physics 16*, 6480-6485.

6. Struder, S. M., and Joseph, S. (2007) Binding of mRNA to the Bacterial Translation Initiation Complex, *Methods in Enzymology 430*, 31-44.

7. Bergqvist, S., Ghosh, G., and Komives, E. A. (2008) The IkBa/NF-kB complex has two hot-spots, one at either end of the interface, *Prot. Sci. 17*, 2051-2058.

8. Mulvihill, M., Guttman, M., and Komives, E. A. (2011) Protein interactions among F65, the low-density lipoprotein receptor-related protein, and the amyloid precursor protein, *Biochemistry-Us 50*, 6208-6216.

9. Sue, S. C., Alverdi, V., Komives, E. A., and Dyson, H. J. (2010) Detection of a ternary complex of NFkB and IkBa with DNA provides insight into how IkBa removes NFkB from transcription sites, *Proc Natl Acad Sci U S A 108*, 1367-1372.

10. Alverdi, V., Hetrick, B., Joseph, S., and Komives, E. A. (2014) Direct observation of a transient ternary complex during IkBa-mediated dissociation of NFkB from DNA, *Proc Natl Acad Sci U S A 111*, 225-230.

11. Huang, T., Kudo, N., Yoshida, M., and Miyamoto, S. (2000) A nuclear export signal in the N-terminal regulatory domain of Ikba controls cytoplasmic localization of inactive NFkB/IkBa complexes, *Proc Natl Acad Sci U S A 97*, 1014-1019.

12. Ourthiague, D., Birnbaum, H., Ortenlof, N., Vargas, J., Wollman, R., and Hoffmann, A. (2015) Limited specificity of IRF3 and ISGF3 in the transcriptional innate-immune response to double-stranded RNA, *J Leuk. Biol. 98*, 119-128.

13. O'Dea, E. L., Barken, D., Peralta, R. Q., Tran, K. T., Werner, S. L., Kearns, J. D., Levchenko, A., and Hoffmann, A. (2007) A homeostatic model of IkappaB metabolism to control constitutive NF-kappaB activity, *Molecular systems biology 3*, 111.

Chapter 4

Predicted Disorder-to-order Transition Mutations in IκBα Disrupt Function

Introduction

Intrinsically disordered proteins have disordered or weakly folded regions and comprise a large portion of the proteome.[1] Often the disordered regions fold upon association to their binding partners, and this coupled folding and binding provides several advantages. Flexibility can allow proteins to conform to the shape of a binding partner thereby increasing complementarily, such as with colicin and TolB.[1] The flexibility can allow the protein to adopt different structures for different binding partners, as is the case with p53, which has been observed in helical, β-strand, or extended structures with different binding partners.[2] Coupled folding and binding can influence the binding kinetics; for example, in the fly-casting mechanism, an unfolded protein binds faster than a well-structured protein because the unfolded protein has a larger capture radius than the folded protein.[3] Simulations on pKID showed that the binding rate could be reduced by increasing the amount of structure in unbound pKID, supporting a fly-casting process.[4]

According to circular dichroism (CD) and amide exchange studies, the last two ankyrin repeats (AR) of IκBα are disordered and are only fully folded when IκBα is bound to NFκB.[5] The weakly folded AR(5-6) region serves as a switch between degradation mechanisms. When IκBα is free, AR5-6 and the C-terminal PEST sequence exposes a degron that targets the protein for a rapid signal- and ubiquitin-independent proteosomal degradation process.[6, 7] This degron is masked when IκBα is bound to NFκB, and the bound protein requires phosphorylation and ubiquitylation at the N-terminal signal response element for targeting to proteosomal degradation.[8] The

switch between degradation mechanisms is accompanied by a large difference in the intracellular half-life of IκBα; free IκBα has a half-life of 10 min, whereas an NFκB-bound IκBα has a half-life of 12 h.[9] The short half-life of free IκBα keeps cellular levels of the inhibitor low, which is essential for robust activation of NFκB. IκBα has a high affinity for NFκB, resulting from an extremely slow dissociation rate.[10] This has been shown to be due in part to the coupled folding and binding of the AR(5-6) region. IκBα inhibits the transcriptional activity of NFκB, and we recently showed that it actually accelerates the dissociation of NFκB from DNA—a process that requires the disordered AR(5-6) region of IκBα.[11]

Alignment of the many hundreds of AR sequences helped to define a consensus sequence, and AR domains that are designed with this consensus in mind are highly stable.[12] We noticed that the more consensus-like ARs of IκBα were AR(1-4), and these had the least amide exchange, whereas AR(5-6) conform less to the consensus and undergo rapid exchange[13] in agreement with lower sequence conservation of the disordered regions. [14] Introduction of two mutations to the consensus sequence in AR6, Y254L and T257A resulted in "pre-folding" of AR6 so that all six ARs became part of the cooperatively folding AR domain (ARD). [15] This mutant had impaired binding affinity and was also less efficient at dissociating NFκB from the DNA.[11, 15]

Here, we searched for another way to find mutations in the weakly folded AR6 of IκBα that might alter folding and function. We used an in-house "Mutator" software (see Materials and Methods) to predict disorder-to-order (D→O) transition mutations in AR6 of IκBα. The algorithm is based on a bioinformatic approach that analyzes

disordered regions of proteins based on sequence information. The "Mutator" predicted two D→O mutations, P261F and E282W, neither of which introduced consensus residues. These mutants were prepared and analyzed for the "foldedness" using amide H/D exchange and CD, for binding to NFκB using SFF following the single tryptophan in AR6 (W258) as a reporter, and for the ability to dissociate NFκB from DNA using SFF following pyrene-labeled DNA. We show that both D→O mutants have slower rate constants for dissociating NFκB from the DNA, emphasizing the functional role for intrinsic disorder in IκBα.

Materials and Methods

Prediction of the disorder-to-order transition mutations

The in-house "Mutator" software was used to predict the D→O transition mutations in the mouse IκBα protein. This software was designed based on the observation that some naturally occurring disease-associated mutations cause a large decrease in the predicted disorder score.[16, 17] The effect of one D → O mutation was verified using accelerated molecular dynamics simulations. In agreement with our predictions, an increased α-helical propensity of the region harboring the mutation was observed.[17] The "Mutator" uses PONDR VL-XT disorder predictor,[18] which assigns the disorder score to each amino acid residue in the protein. The ''Mutator'' automatically replaces each residue within a user-defined window with each of the 19 remaining residues and recalculates PONDR VL-XT scores after each change. Subsequently, to suggest the mutation for mutagenesis, the ''Mutator'' calculates the

area under the prediction curve (AUC) and suggests the mutation that causes the largest decrease of the AUC. Since the disorder score is calculated based on the sliding window, a change of one amino acid influences the disorder score of the entire region. According to VL-XT prediction, full-length human IκBα has two long disordered regions: residues 1–68 and 253–298, with the latter interspersed by a short, ordered segment. It also has two short disordered regions, 81–92 and 254–262. The region 253–298, containing AR5–AR6 and the PEST was selected for mutagenesis in this study. Two mutations in IκBα, which caused the largest difference in the AUC, P261F and E282W, were selected as candidates for experimental confirmation.

Protein expression and purification

Human wild-type IκBα$_{67-287}$ referred to simply as IκBα and mutants (P261F and E282W) were expressed in *E. coli* BL21 DE3 cells and purified using a Hi-Load Q Sepharose (GE Healthcare, Pittsburgh, PA, USA) followed by a Superdex 75 column (GE Healthcare) as described previously.[10, 13] The protein concentrations were determined by spectrophotometry (ε IκBα WT and P261F = 12,950 M^{-1}cm^{-1}, and ε IκBα E282W = 18,450 M^{-1}cm^{-1}).

The N-terminal hexahistidine-NFκB (His$_6$-p50$_{39-350}$/RelA$_{19-321}$) heterodimer was co-expressed using the method described previously[19] and purified by nickel affinity chromatography (Ni-NTA Agarose, Qiagen, Valencia, CA, USA), cation exchange chromatography (Mono S column, GE Healthcare), and size exclusion chromatography (Superdex 200, GE Healthcare). The protein concentration was determined by spectrophotometry (ε NFκB = 43,760 M^{-1}cm^{-1}).

Murine RelA$_{190-321}$ with an N-terminal cysteine, and murine p50$_{248-350}$, were expressed, purified, and quantified as described.[10] The RelA$_{190-321}$ dimerization domain, RelA$_{190-321}$ in 25 mM Tris pH 7.2, 150 mM NaCl, 1 mM EDTA was biotinylated by incubation with a 1:1 molar ratio of biotin PEO maleimide (Pierce Chemicals), neutation at room temperature for 1 h, and purification immediately by size exclusion chromatography on a S75 Superdex 16/60 column at 4 °C in SPR Immobilization Buffer (SPR-IB) (500 mM NaCl, 10 mM Tris pH 7.5, 0.5 mM EDTA, 0.5 mM sodium azide, 0.005% v/v P20). Murine p50$_{248-350}$ was purified by size exclusion chromatography as above. To form the (p50$_{248-350}$/RelA$_{190-321}$) heterodimer, referred to as biotinylated NFκB, a 50-fold excess of unbiotinylated p50$_{248-350}$ was incubated with biotin-RelA$_{190-321}$ at room temperature for 1 h and subsequently at 4 °C overnight.

Hydrogen/deuterium exchange mass spectrometry

Hydrogen/deuterium exchange mass spectrometry (HDXMS) was performed using Waters nanoACQUITY UPLC system with H/DX technology (at Lilly, Inc. San Diego). For each different deuteration time, 5 µL of purified protein ([WT] = 84 µM, [E282W] = 82 µM and [P261F] = 90 µM) was mixed with 55 µL of D$_2$O buffer (containing 0.1X PBS) for a specified amount of time (0 s to 10 min) at 15 °C. The exchange was quenched for 2 min at 1 °C with an equal volume of 100 mM phosphate with 320 mM TCEP (pH 2.4). The quenched sample was injected into a 50 µL sample loop, followed by on-line pepsin column digestion (Applied Biosystems, Poroszyme

Immobilized Pepsin cartridge). The resulting peptic peptides were captured on a Vanguard trap column, separated by analytical column (Waters, Acquity UPLC BEH C18, 1.7 µm, 1.0x50 mm) with a gradient of 3%–85% acetonitrile in 12 min where both mobile phases contained 0.2% formic acid, and directed into a Waters SYNAPT G2 quadrupole time-of-flight mass spectrometer. The mass spectrometer was set to collect data in the MS^E, ESI+ mode; mass acquisition range of 255.00 - 1950.00 (m/z); scan time 0.4 s. Continuous lock mass correction was accomplished with infusion of a peptide standard every 30 s (mass accuracy of 1 ppm for calibration standard). The peptides were initially identified by using PLGS 2.5 (Waters, Inc.) with a mass accuracy of 3-5 ppm and fragmental ions, and the relative deuterium uptake for each peptide was calculated by comparing the centroids of the mass envelopes of the deuterated samples with the undeuterated controls using DynamX 2.0 (Waters Corporation). Details of this methodology have been previously reported.[20]

Circular dichroism spectroscopy

CD measurements were performed with an Aviv 202 spectropolarimeter (Aviv Biomedical, Lakewood, NJ). The proteins were dissolved in 10 mM NaHPO$_4$ pH 7.5, 150 mM NaCl, 1 mM DTT, 0.5 mM EDTA at a concentration of 60 µM except for the E282W which was at 55 µM. All the spectra were collected at a constant temperature of 25 °C. The uncorrected ellipticity is reported. IκBα

SPR experiments

Sensorgrams were recorded on a Biacore 3000 instrument using streptavidin chips (GE Healthcare). Biotinylated NFκB was immobilized in SPR-IB on flow cell (FC) 2, FC 3, and FC 4 with 50, 100, and 150 RU, respectively, leaving FC 1 unmodified. Data were collected at the high collection rate on FCs 2, 3, and 4 automatically subtracting FC 1. Binding experiments were conducted on IκBα, IκBα P261F, IκBα E282W, and IκBα E282Q in SPR Running Buffer (SPR-RB) (50 mM Tris pH 7.5, 150 mM NaCl, 1 mM EDTA, 0.5 mM sodium azide, 10% w/v glycerol, 0.005% P20) at 50 μL/min using the kinject function with a 5 min contact time and a 20 min dissociation. The surface was regenerated by a 1 min pulse of 1.5 M urea diluted from a 6 M stock in SPR-RB. The data were analyzed as previously described.[21]

Stopped-flow fluorescence

To measure the association of IKBA to NFκB or to the NFκB-DNA complex, we took advantage of the native Trp fluorescence of IκBα W258. Six different concentrations of NFκB or of the NFκB-DNA complex (0.3, 0.4, 0.5, 0.6, 0.7, 0.8 μM) were mixed with IκBα (0.1 μM). All stopped-flow kinetic experiments were performed at 25 °C using an SX-20 stop-flow apparatus (Applied Photophysics, Leatherhead, UK) set to collect 2000 pt linearly with a final mixing volume of 200 μL. Twenty traces were collected for each concentration, and 10 traces that overlaid well were selected and averaged. The data were processed using pro Fit 6.1.14 and were fit to a single exponential. The observed association rates were plotted against the IκBα

concentration and fit using a linear model to obtain the association rate constant. We did not observe any difference in the fluorescence change for the E282W as compared to wild type IκBα even though this mutation introduces a second Trp. We believe this is because position 282 is at the very C-terminus of the protein in a relatively solvent-exposed region.

To measure the IκBα-mediated dissociation of DNA from NFκB we used a hairpin DNA sequence corresponding to the IFNκB site, 5'-AmMC6/GGGAAATTCCTCCCCCAGGAATTTCCC-3' (IDT Technologies, Coranville, CT, USA), which was labeled with pyrene (N-hydroxyl succinimide ester) and is referred to as DNA^P, as described.[22] The pyrene was excited at 343 nm, and the fluorescence emission was monitored at 376 nm with a cut-off filter at 350 nm. Fluorescence of the naturally-occurring IκBα W258 was followed by exciting at 280 nm and monitoring the emission at 345-355 nm with a cut-off filter at 320 nm. The rate of IκBα-mediated dissociation of the DNA from NFκB was measured by adding different concentrations of IκBα (0.25, 0.5, 0.75, 1, 1.25, 1.5, 1.75, and 2 µM) to a 1 µM NFκB:1.2 µM DNA^P complex. The curves were fitted with pro Fit 6.1.14 using a single exponential dissociation model. The observed dissociation rates were plotted against the IκBα concentration and fit using a linear model to obtain the rate constant for IκBα-mediated dissociation of the NFκB-DNA complex.

All of the experiments reported above were repeated using IκBα P261F and IκBα E282W (and for some E282Q) in place of the wild type IκBα. NFκB

Results

Predicting disorder-to-order transitions in IκBα using the "Mutator" algorithm

IκBα 67–287 has increased intrinsic disorder towards the C-terminus of the protein (Figure 4.1). According to VL-XT prediction, the IκBα ARD has a long disordered region extending from residue 253 to residue 298 interspersed by a short ordered segment, and this region was selected for mutagenesis in this study. Two mutations in IκBα, P261F and E282W, were predicted to increase order of the C-terminal disordered region of the protein (Figure 4.1A). It is interesting to note that when we analyzed the mutations that were known to stabilize IκBα based on mutation to the stable ankyrin repeat consensus sequence, these mutations did not result in predicted ordering of the 253–298 region according to the VL-XT prediction, possibly because this region is initially predicted as ordered by the VL-XT (Figure 4.1B). These results demonstrate that the disorder predictor accesses a different realm of protein folding space than the consensus sequence, which is was our aim in this approach.
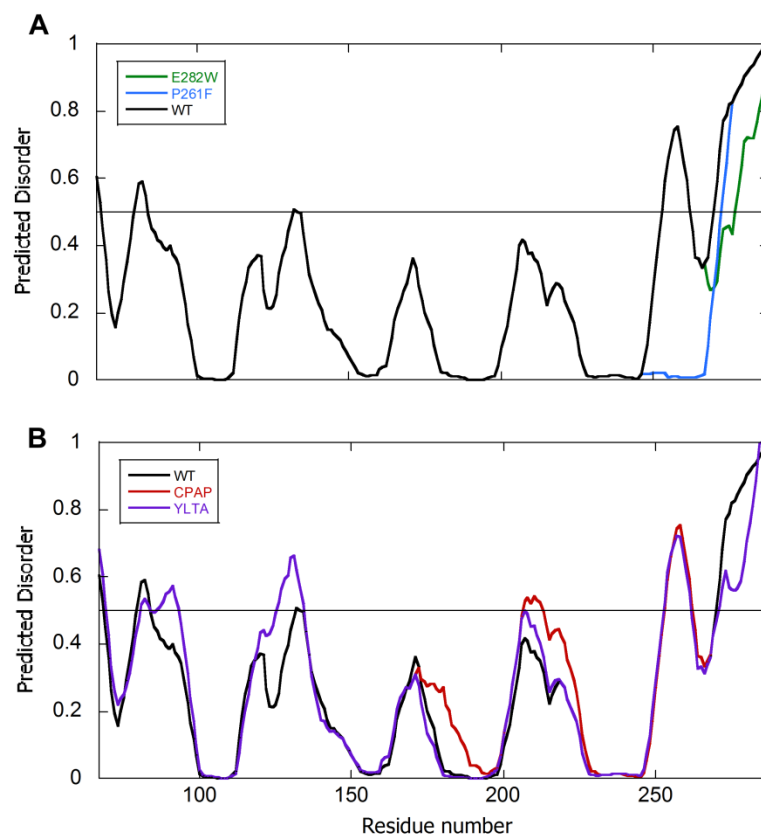
Figure 4.1. Plot of the PONDR VL-XT predicted disorder for the ARD (residues 67-287) of IκBα WT and mutants. The score of ≥ 0.5 signifies predicted disorder, whereas the score of <0.5 signifies predicted order (depicted by the horizontal line in each figure). (A) IκBα WT (black), IκBα P261F (blue), and IκBα E282W (green). The P261F mutant is predicted to be more ordered in residues 249-265, whereas the E282W mutant is predicted to be more ordered in residues 270-287. (B) IκBα WT (black), IκBα C186P/A220P (red), and IκBα Y254L/T257A (purple). The C186P/A220P and the Y254L/T257A mutations do not influence the disorder score of the region 253-298, except for a slight increase in disorder in the 207-212 region for the C186P/A220P mutant.

Assessment of the "foldedness" of the D→O mutants

We previously showed that all of the amides in AR5 and AR6 of IκBα exchange rapidly, whereas the amides in AR(1-4) exchange much more slowly.[13] We interpreted the differential exchange behavior in light of folding simulations that indicated AR(1-4) formed a stable, folded, domain whereas AR(5-6) folded later and more weakly.[23] In fact, the consensus YLTA mutant showed significantly reduced exchange in AR5 and AR6.[15] A similar approach was used to assess whether the D→O mutant proteins were more well-folded. The wild type and each mutant protein were incubated in deuterated buffer for 0-10 min, and the amide exchange was assessed after quench and pepsin digestion by mass spectrometry.[13] We were only able to accurately assess the foldedness of the E282W mutant; however, because the P261F mutation introduced a pepsin cleavage site that resulted in a different distribution of peptides, P261F could not be directly compared to the wild type. Three peptides showed slightly reduced exchange in the E282W mutant, but the only one with significantly reduced exchange was the peptide that covered the site of the mutation (Figure 4.2). Thus, amide exchange indicates that at least for the E282W mutant, introduction of this single, non-consensus mutation, which was predicted only a bioinformatics algorithm, results in a more folded conformation.
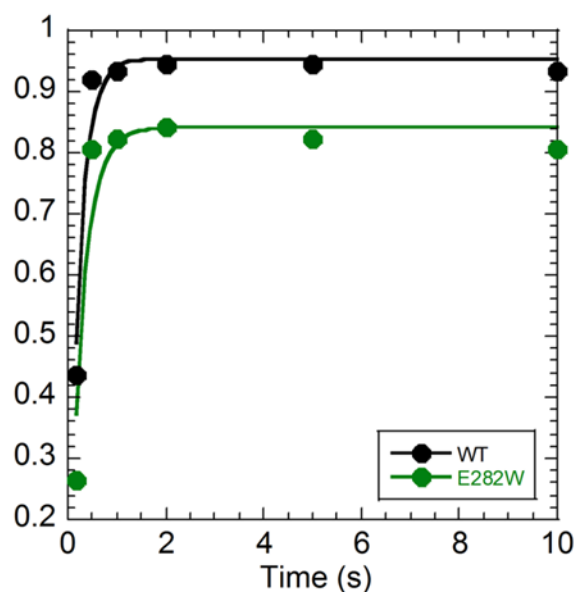
Figure 4.2. Amide H/D exchange for the E282W D→O mutant. The C-terminal residues showed reduced exchange in the E282W mutant (green) compared to wild type IκBα (black).

To further explore the possible ordering introduced by the D→O mutations, we measured the ellipticity by circular dichroism (CD) of equal concentrations of wild type, P261F, E282W, and a control mutant, E282Q. The E282W mutant showed a significant increase in helical signal, whereas the P261F and E282Q mutants had the same helical content as wild type IκBα (Figure 4.3). Thus, both CD and amide exchange indicated a slight increase in ordered structure for the E282W mutant.
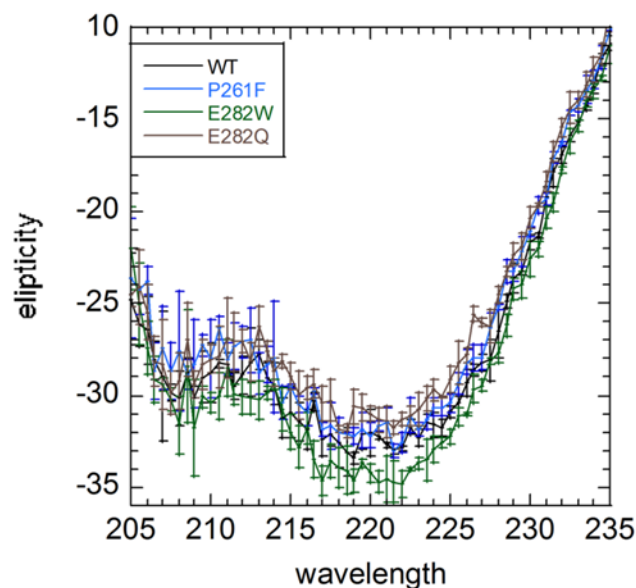
Figure 4.3. Circular dichroism spectroscopy of IκBα WT and mutants. CD showed a statistically significant increase in helicity for the E282W mutant, but not for the P261F mutant. Error bars are the standard deviation from three independent experiments.

Effect of D→O mutations in IκBα on binding kinetics

To assess whether the mutations affected the kinetics of binding of the mutant IκBα proteins to NFκB (p50/RelA), we used both SPR and SFF. For the stopped-flow experiments, we monitored the change in fluorescence of the naturally-occurring Trp258 in AR6 of IκBα that increases fluorescence upon binding.[24] The P261F mutant bound with the same association rate constant as the wild type ($1.4 \ (\pm 0.1) \times 10^7$ M^{-1} s^{-1}), and the E282W mutant showed a slight decrease in binding rate ($1.1 \ (\pm 0.1) \times 10^7$ M^{-1} s^{-1}) (Figure 4.4).
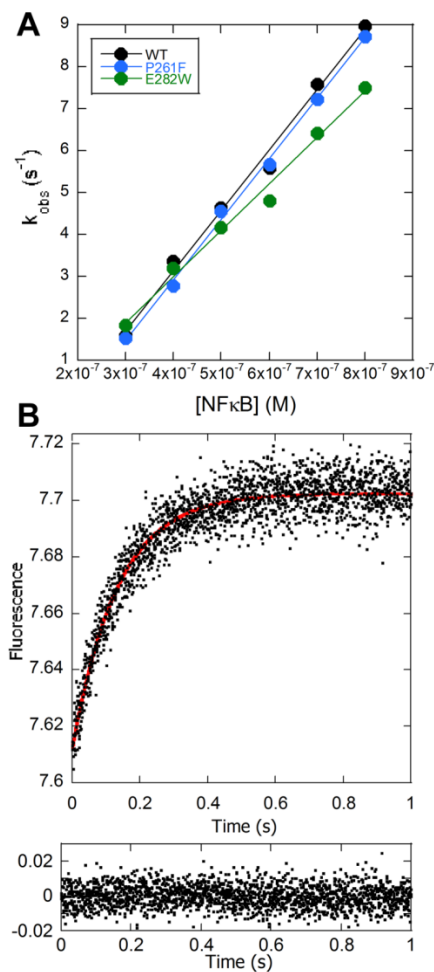
Figure 4.4. SFF IκBα binding experiments to NFκB show that IκBα WT, P261F, and E282W show similar association rates to NFκB. SFF kinetic experiments in which IκBα (0.1 μM) was mixed with varying concentrations of NFκB, and the change in intensity of the Trp fluorescence from the native W258 in IκBα was monitored. (A) Plot of the fluorescence relaxation times determined at constant IκBα concentration and varying NFκB concentrations, which could be linearly fit yielding the association rate constant. (B) A representative SFF trace obtained by mixing 0.1 μM IκBα with 0.8 μM NFκB is shown with the corresponding residuals for the single exponential fit (red line in trace) plotted below the trace.

We could not measure dissociation by stopped-flow because the NFκB-IκBα complex binds extremely tightly; however, the SPR results showed similar dissociation rates and relatively similar K_D's of 172 ± 4 pM for WT, 462 ± 8 pM for P261F, and 155 ± 14 pM for the E282W mutant (Figure 4.5 and Table 4.1). Although P261F binds to NFκB slightly more weakly than WT IκBα, its K_D still exhibits the strong binding associated with the IκBα-NFκB complex. Furthermore, we found no correlation between binding affinity and the rate at which the IκBα variants dissociated NFκB from DNA.

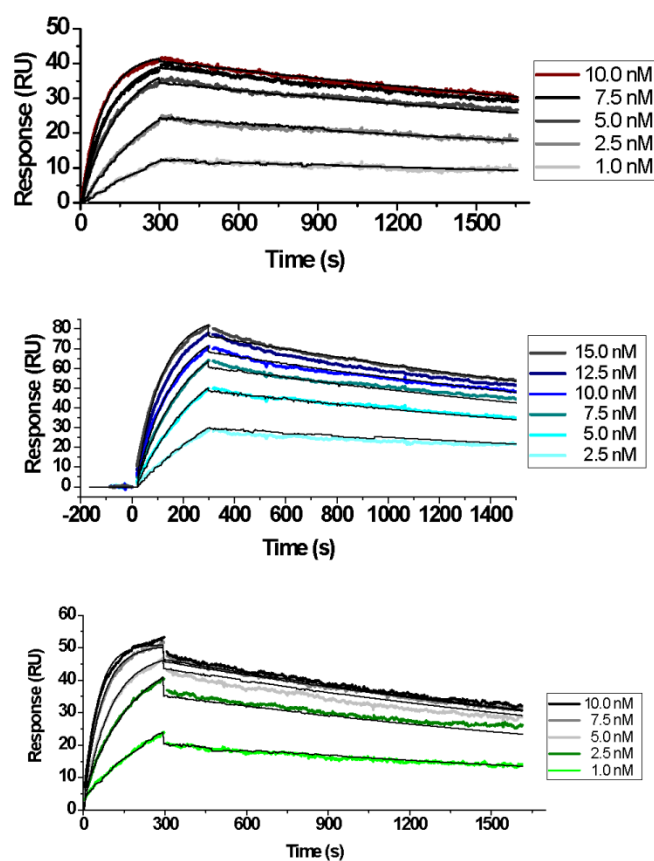**Figure 4.5**. **SPR traces for binding of IκBα WT and the D→O mutants to p50dd/biotin-p65dd.** The binding constants for wild type (black), the P261F mutant (blue) and the E282W mutant (green) derived from these plots are given in Table 4.1.

Table 4.1. Kinetic rates derived from SPR experiments of IκBα binding to biotin-NFκB.

	k_a ($M^{-1}s^{-1}$)		k_d (M^{-1})		K_D (M)	
	Average	Standard Deviation	Average	Standard Deviation	Average	Standard Deviation
IκBα WT	1.2E+06	3.1E+04	2.1E-04	6.7E-06	1.7E-10	4.0E-12
P261F	6.9E+05	3.4E+04	3.2E-04	1.4E-05	4.6E-10	8.2E-12
E282W	2.0E+06	1.0E+05	3.0E-04	7.2E-06	1.6E-10	1.4E-11
E282Q	5.5E+06	6.2E+05	5.0E-04	2.0E-05	9.2E-11	1.2E-11

Effect of disorder-to-order mutations in IκBα-mediated dissociation of NFκB from DNA

We previously showed that introduction of consensus mutations that stabilize the ARD of IκBα decreases the rate constant for IκBα-mediated dissociation of NFκB from DNA.[11] We used SFF to follow how well the non-consensus D→O mutant IκBαs mediated dissociation of DNA^P from the NFκB-DNA^P complex as described previously.[24] Both mutants showed decreased rate constants for IκBα mediated dissociation of NFκB from DNA^P. Wild type IκBα facilitated dissociation with a second order rate constant of 2.3 (±0.1) x 10^6 M^{-1} s^{-1}, whereas the rate constant for the P261F mutant was 1.8 (±0.1) x 10^6 M^{-1} s^{-1}, a decrease of 22%, and the rate constant for the E282W mutant was 1.6 (±0.1) x 10^6 M^{-1} s^{-1}, a decrease of 30% (Figure 4.6). While these differences were small, they were statistically significant and reproducible across several experiments and with different protein preparations.
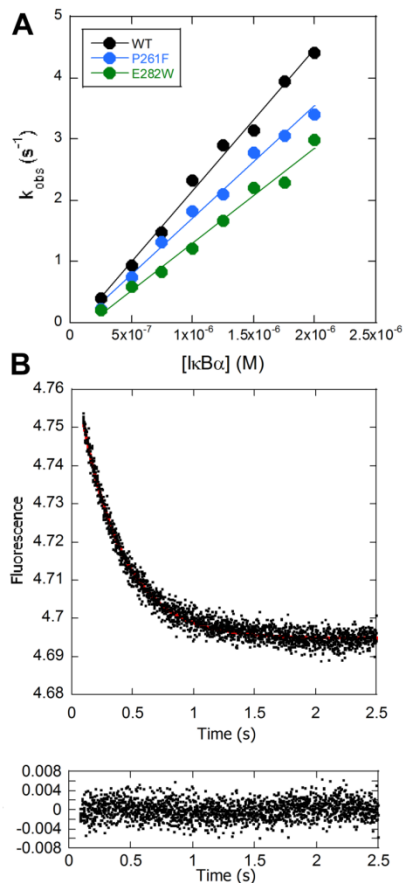
Figure 4.6. The IκBα D→O mutants are deficient in mediating the dissociation of NFκB from DNA[P]**.** SFF was used to measure the dissociation of DNA[P] from the NFκB- DNA[P] complex in the presence of varying concentrations of IκBα. Upon binding of IκBα to the NFκB-DNA complex, the fluorescence increased in the first 100 ms and then decreased to the values expected for free DNA[P]. The IκBα-concentration-dependent dissociation rate was measured from the second part of the traces. (A) The dissociation became more rapid with increasing IκBα concentration, and the plot of the fluorescence relaxation times vs. IκBα concentrations could be fit linearly yielding the second order rate constant for IκBα mediated dissociation of the NFκB- DNA[P] complex. (B) A representative stopped flow trace obtained by mixing 0.1 μM NFκB-DNA[P] complex with 1.25 μM IκBα is shown with the corresponding residuals for the single exponential fit (red line in trace) plotted below the trace.

To control for the change in charge of the E282W mutant, we also measured the rate constant for the E282Q mutant. Compared to wild type IκBα, this mutant had the same predicted disorder and a rate constant of 2.2 ($\pm$0.1) x 10^6 M^{-1} s^{-1} that is nearly identical to the wild type protein (Figure 4.7).
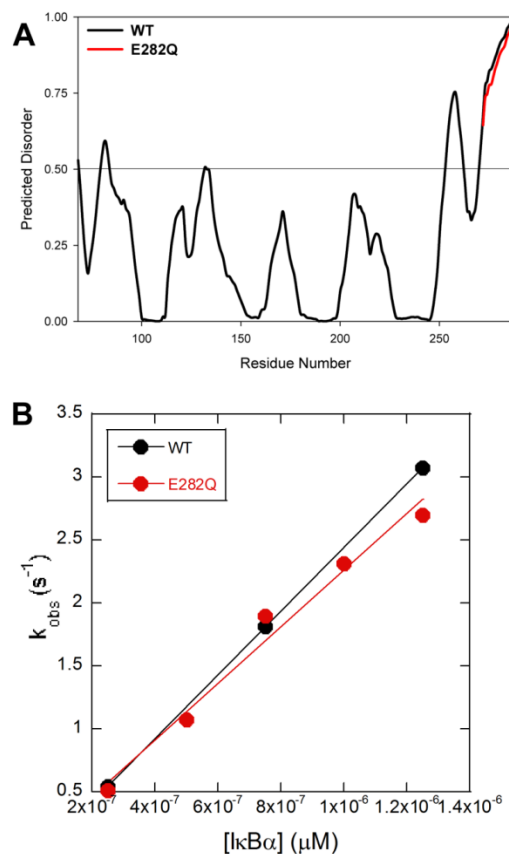
Figure 4.7. Control studies were performed with the IκBα E282Q mutant. (A) This mutation was not predicted to impart order. (B) The E282Q mutant had a second order rate constant for dissociating NFκB from DNA equivalent to that of the IκBα WT.

To determine whether the decreased second order rate constant for dissociating NFκB from the DNA was due to decreased association of the mutant IκBαs with the NFκB-DNA complex, the first step in the facilitated dissociation, we measured the association of each IκBα to the NFκB-DNA complex, again by following the change in fluorescence of the Trp258 in IκBα. The wild type IκBα associated with the NFκB-DNA complex with a rate constant of 4.4 (±0.1) x10^6 M^{-1} s^{-1}, the P261F mutant rate constant was 4.0 (±0.3) x 10^6 M^{-1} s^{-1}, a decrease of 9%, and the E282W rate constant was 3.8 (±0.3) x 10^6 M^{-1} s^{-1}, a decrease of 14%. These results show that association accounts for some, but not all of the decrease (Figure 4.8). Thus, the mutants appear to be less able to actually facilitate dissociation of the DNA after the transient ternary complex is formed.
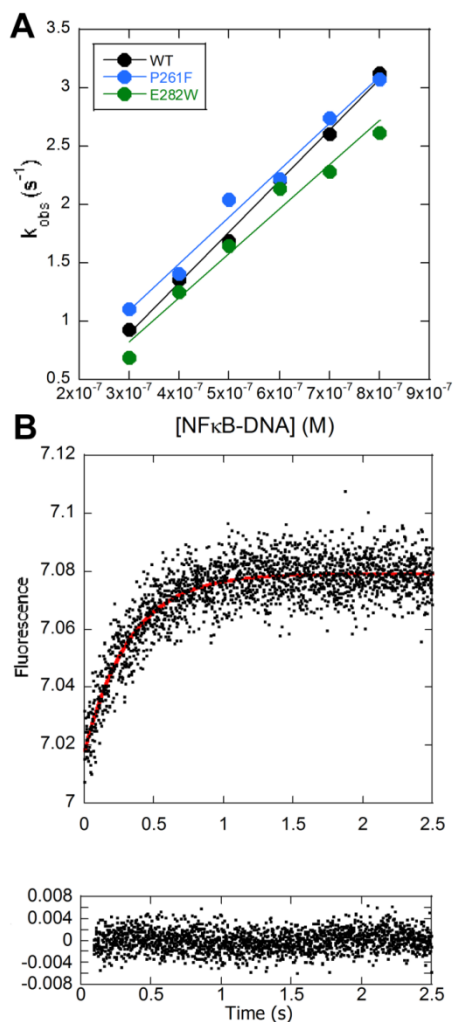
Figure 4.8. SFF kinetic experiments show that the D→O mutants bind to the NFκB-DNA complex with high affinity. IκBα (0.1 μM) was mixed with varying concentrations of NFκB-DNA complex and the change in intensity of the Trp fluorescence from the native W258 in IκBα was monitored. (A) Plot of the fluorescence relaxation times determined at constant IκBα concentration and varying NFκB-DNA complex concentrations. The linear fit yielded the association rate constant. (B) A representative SFF trace of IκBα (0.1 μM) mixed with the NFκB-DNA complex (1.25 μM) and the single exponential fit (red line in trace). The corresponding residuals for the single exponential fit are shown below the trace.

Discussion

In conclusion, we have used a bioinformatic-based algorithm to predict D→O mutations in the intrinsically disordered C-terminal region of IκBα. Two mutations were predicted to cause the largest D→O transition in this region, and both were tested. To examine changes in "foldedness," amide H/D exchange and CD spectroscopy were used. Only the E282W mutant showed decreased amide exchange that was significant in residues 278-287, precisely the residues that were predicted to transition to a more ordered state by the "Mutator" algorithm. This mutant also showed a significant increase in helicity by CD spectroscopy, further corroborating that this mutant is more well-folded.

We had previously shown that mutations towards the consensus for stable ankyrin repeats decreased the rate constant for IκBα-mediated dissociation of NFκB from DNA.[11] Here we attempted to access more ordered conformations by an alternative approach—the "Mutator" algorithm. Interestingly, when the algorithm was used to predict ordering for the consensus mutants (i.e., IκBα C186P/A220P and IκBα Y254L/T257A), suggesting that consensus mutation and purely sequence-based predictions provide alternative approaches to introducing order to foldedness, vaguely defined in ankyrin repeat domains. Both D→O mutations decreased the rate constant for IκBα-mediated dissociation of NFκB from DNA; however, the E282W mutation had a stronger effect. This observation emphasizes the requirement for disorder in IκBα to efficiently dissociate NFκB from DNA and suggests that the defective dissociation of the consensus mutations was indeed due to their ordering of the

disordered AR(5-6) of IκBα. While the D→O mutants affected the association of the mutant IκBαs to the NFκB-DNA complex, these mutations more strongly affected the rate of IκBα–mediated dissociation. The results emphasize how perfectly tuned the IκBα energy landscape is for the function of dissociating NFκB from the DNA.

Acknowledgements

Chapter 4, in full, is a reprint of which the dissertation author was the principal researcher and author. The material appears in *Physical Chemistry Chemical Physics*. (**Dembinski, H.**, Wismer, K., Balasubramaniam, D., Gonzalez, H., Alverdi, V. Iakoucheva, L.M., Komives, E.A. (2014). Predicted disorder-to-order transition mutations in IκBα disrupt function. *Physical Chemistry Chemical Physics,* **16**, 6480-6485.)

References

1.   Wright, P. E., and Dyson, H. J. (2009) Linking folding and binding, *Current opinion in structural biology 19*, 31-38.

2.   Oldfield, C. J., Meng, J., Yang, J. Y., Yang, M. Q., Uversky, V. N., and Dunker, A. K. (2008) Flexible nets: disorder and induced fit in the associations of p53 and 14-3-3 with their partners, *BMC Genomics 9 Suppl 1*, S1.

3.   Shoemaker, B. A., Portman, J. J., and Wolynes, P. G. (2000) Speeding molecular recognition by using the folding funnel: the fly-casting mechanism, *Proceedings of the National Academy of Sciences of the United States of America 97*, 8868-8873.

4.   Turjanski, A. G., Gutkind, J. S., Best, R. B., and Hummer, G. (2008) Binding-induced folding of a natively unstructured transcription factor, *PLoS Comput Biol 4*, e1000060.

5.   Truhlar, S. M., Torpey, J. W., and Komives, E. A. (2006) Regions of IkappaBalpha that are critical for its inhibition of NF-kappaB.DNA interaction fold upon binding to NF-kappaB, *Proceedings of the National Academy of Sciences of the United States of America 103*, 18951-18956.

6.   Mathes, E., O'Dea, E. L., Hoffmann, A., and Ghosh, G. (2008) NF-kappaB dictates the degradation pathway of IkappaBalpha, *The EMBO journal 27*, 1357-1367.

7.   Mathes, E., Wang, L., Komives, E., and Ghosh, G. (2010) Flexible regions within I{kappa}B{alpha} create the ubiquitin-independent degradation signal, *J Biol Chem 285*, 32927-32936.

8.   Ghosh, S., May, M. J., and Kopp, E. B. (1998) NF-kappa B and Rel proteins: evolutionarily conserved mediators of immune responses, *Annual review of immunology 16*, 225-260.

9.   O'Dea, E. L., Barken, D., Peralta, R. Q., Tran, K. T., Werner, S. L., Kearns, J. D., Levchenko, A., and Hoffmann, A. (2007) A homeostatic model of IkappaB metabolism to control constitutive NF-kappaB activity, *Molecular systems biology 3*, 111.

10. Bergqvist, S., Croy, C. H., Kjaergaard, M., Huxford, T., Ghosh, G., and Komives, E. A. (2006) Thermodynamics reveal that helix four in the NLS of NF-kappaB p65 anchors IkappaBalpha, forming a very stable complex, *J. Mol. Biol. 360*, 421-434.

11. Bergqvist, S., Alverdi, V., Mengel, B., Hoffmann, A., Ghosh, G., and Komives, E. A. (2009) Kinetic enhancement of NF-kappaBxDNA dissociation by IkappaBalpha, *Proceedings of the National Academy of Sciences of the United States of America 106*, 19328-19333.

12. Binz, H. K., Stumpp, M. T., Forrer, P., Amstutz, P., and Pluckthun, A. (2003) Designing repeat proteins: well-expressed, soluble and stable proteins from combinatorial libraries of consensus ankyrin repeat proteins, *J Mol Biol 332*, 489-503.

13. Croy, C. H., Bergqvist, S., Huxford, T., Ghosh, G., and Komives, E. A. (2004) Biophysical characterization of the free IkappaBalpha ankyrin repeat domain in solution., *Protein Sci. 13*, 1767-1777.

14. Brown, C. J., Johnson, A. K., and Daughdrill, G. W. (2010) Comparing models of evolution for ordered and disordered proteins, *Mol Biol Evol 27*, 609-621.

15. Truhlar, S. M., Mathes, E., Cervantes, C. F., Ghosh, G., and Komives, E. A. (2008) Pre-folding IkappaBalpha alters control of NF-kappaB signaling, *J Mol Biol 380*, 67-82.

16. Vacic, V., and Iakoucheva, L. M. (2012) Disease mutations in disordered regions-exception to the rule?, *Mol Biosyst 8*, 27-32.

17. Vacic, V., Markwick, P. R., Oldfield, C. J., Zhao, X., Haynes, C., Uversky, V. N., and Iakoucheva, L. M. (2012) Disease-associated mutations disrupt functionally important regions of intrinsic protein disorder., *PLoS Comput Biol*, 8: e1002709.

18. Li, X., Romero, P., Rani, M., Dunker, A. K., and Obradovic, Z. (1999) Predicting protein disorder for N-, C-, and internal regions, *Genome Informatics Series Workshop 10*, 30-40.

19. Sue, S. C., Cervantes, C., Komives, E. A., and Dyson, H. J. (2008) Transfer of flexibility between ankyrin repeats in IkappaB* upon formation of the NF-kappaB complex, *J Mol Biol 380*, 917-931.

20. Wales, T. E., Fadgen, K. E., Gerhardt, G. C., and Engen, J. R. (2008) High-speed and high-resolution UPLC separation at zero degrees Celsius, *Anal Chem 80*, 6815-6820.

21. Bergqvist, S., Ghosh, G., and Komives, E. A. (2008) The IkappaBalpha/NF-kappaB complex has two hot spots, one at either end of the interface, *Protein Sci 17*, 2051-2058.

22. Studer, S. M., and Joseph, S. (2007) Binding of mRNA to the Bacterial Translation Initiation Complex, *Meth Enzymol 430*, 31-44.

23. Ferreiro, D. U., Cho, S. S., Komives, E. A., and Wolynes, P. G. (2005) The energy landscape of modular repeat proteins: topology determines folding mechanism in the ankyrin family., *J Mol Biol. 354*, 679-692.

24. Alverdi, V., Hetrick, B., Joseph, S., and Komives, E. A. (2014) Direct observation of a transient ternary complex during IκBα-mediated dissociation of NF-κB from DNA., *Proceedings of the National Academy of Sciences of the United States of America 111*, 225-230.

Chapter 5

Global Stabilization of NFκB upon DNA Binding

Introduction

While the majority of the present work has focused on the role of IκBα in regulating NFκB, many questions remain unanswered regarding the functional dynamics of NFκB. For example, from the DNA-binding vantage, it has been shown that NFκBs can bind strongly to specific κB DNA sequences (K_D = 3 nM) and that different NFκBs have varying affinities for different κB sites, yet NFκBs can also bind to non-specific sites with affinity relatively high for transcription factors ($K_D \approx 50$ nM)[1-3]. Additionally, it has been shown that the cellular composition and transcriptional activity of NFκB dimers can be heavily influenced by the presence IκBs; simultaneously, however, the canonical IκBα rapidly mediates the dissociation of NFκB from DNA.[4] For example, one hypothesis put forward recently is the "chaperone" hypothesis which suggests that IκBs may preferentially stabilize certain homo- or heterodimeric NFκBs and subsequently, therefore, influence which genes are activated upon cellular stimulation. At least in one case, it was recently shown that IκBβ is required for stabilization of RelA (p65) homodimers.[5] These observations lead one to consider the influence of each of these binding partners on NFκB dynamics.

In an effort to obtain biophysical data to better understand NFκB stabilization, we are currently investigating the dynamics of p50/p65 NFκB in each of the stages of NFκB transcriptional activity and regulation by IκBα—free NFκB, NFκB binding to DNA, NFκB in the ternary complex, and NFκB in complex with IκBα. Here we

present a preliminary glimpse into the dynamics and function of NFκB binding to DNA as monitored by thermal denaturation and HDXMS.

Materials and Methods

Protein expression and purification

Murine, N-terminal hexahistidine-p50$_{39–350}$/RelA$_{19–321}$ heterodimer (NFκB) was co-expressed as described previously[6] and purified by nickel affinity chromatography (Ni-NTA Agarose, Qiagen, Valencia, CA, USA), cation exchange chromatography (Mono S column, GE Healthcare), and size exclusion chromatography (Superdex 200, GE Healthcare).

A hairpin DNA sequence corresponding to the IFN-κB site 5'-GGGAAATTCCTCCCCCAGGAATTTCCC-3' was purchased (IDT Technologies, Coranville, CT, USA).

Circular dichroism thermal melts

Circular dichroism (CD) measurements were performed on an Aviv 202 spectropolarimeter (Aviv Biomedical, Lakewood, NJ) with 10 µM NFκB and 20 µM DNA in 10 mM NaHPO$_4$ pH 7.5, 150 mM NaCl, 1 mM DTT, 0.5 mM EDTA. CD signal was monitored at 225 nm with a temperature range from 25 °C to 80 °C with 0.5 °C step, 5 s averaging time, and 0.1 min equilibration.

Hydrogden/deuterium exchange mass spectrometry

Hydrogen/deuterium exchange mass spectrometry (HDXMS) was performed using Waters nanoACQUITY UPLC system with H/DX technology. The NFκB (5 µM) and NFκB (5 µM)-DNA (50 µM) samples in 25 mM Tris pH 7.5, 150 mM NaCl, 1 mM DTT, 0.5 mM EDTA. For each deuteration time, 4 µL free NFκB or NFκB-DNA complex were equilibrated to 25 °C for 5 min and then mixed with 56 µL D_2O buffer (25 mM Tris pH 7.5, 150 mM NaCl, 1 mM DTT, 0.5 mM EDTA in D_2O) for 0, 0.5, 1, 2, 5, or 10 min. The exchange was quenched with an equal volume of quench solution (3 M guanidine, 0.1% formic acid, pH 2.66). The quenched sample was then injected into the 50 µL sample loop, followed by digestion on an in-line pepsin column (immobilized pepsin, Pierce, Inc.) at 15°C. The resulting peptides were captured on a BEH C18 Vanguard pre-column, separated by analytical chromatography (Acquity UPLC BEH C18, 1.7 µM, 1.0 X 50 MM, Waters Corporation) using a 7-85% acetonitrile in 0.1% formic acid over 7.5 min, and electrosprayed into the Waters SYNAPT G2Si quadrupole time-of-flight mass spectrometer. The mass spectrometer was set to collect data in the Mobility, ESI+ mode; mass acquisition range of 200–2,000 (m/z); scan time 0.4 s. Continuous lock mass correction was accomplished with infusion of leu-enkephalin (m/z = 556.277) every 30 s (mass accuracy of 1 ppm for calibration standard). For peptide identification, the mass spectrometer was set to collect data in MS^E, ESI+ mode instead. The peptides were identified from triplicate analyses of 10 µM NFκB, and data were analyzed using PLGS 2.5 (Waters Corporation). Peptides masses were identified using a minimum number of 250 ion counts for low energy peptides and 50

ion counts for their fragment ions; the peptides also had to be larger than 1500 Da. The following cut-offs were used to filter peptide sequence matches: minimum products per amino acid of 0.2, minimum score of 8, maximum MH+ error of 3 ppm, a retention time standard deviation of 5%, and the peptides had to be present in all three ID runs. The peptides identified in PLGS were then analyzed in DynamX 3.0 (Waters Corporation). The relative deuterium uptake for each peptide was calculated by comparing the centroids of the mass envelopes of the deuterated samples with the undeuterated controls following previously published methods.[7]

Results

NFκB-DNA complex exhibits increased thermal stability over free NFκB

To determine whether DNA binding affects the stability of NFκB, free NFκB and the NFκB-DNA complex were subjected to thermal denaturation while monitoring the α-helical signal of NFκB at 225 nm. As can be seen in Figure 5.1, free NFκB underwent a folded to unfolded transition at 47 °C, whereas the NFκB-DNA complex underwent a folded-to-unfolded transition at 73 °C. This marked stabilization was wholly unexpected and led to further investigation of the structural changes within NFκB upon DNA binding.
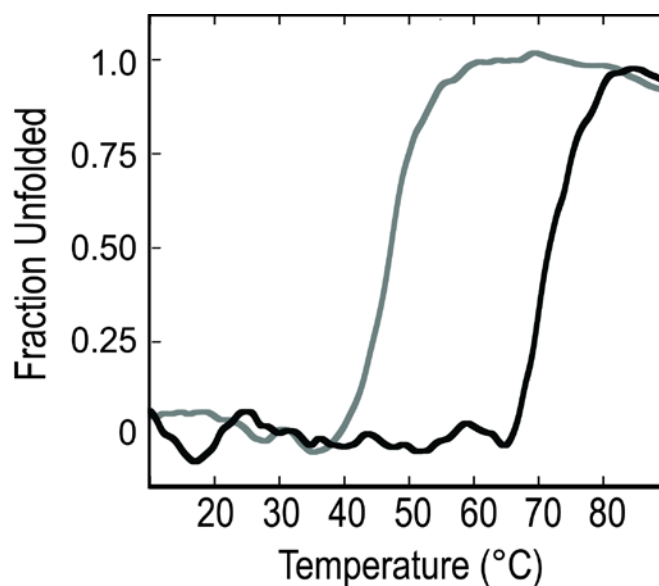

Figure 5.1. Thermal denaturation suggests that NFκB exhibits increased stability due to DNA binding. Circular dichroism signal at 225 nm as a function of temperature monitoring the foldedness of free NFκB (gray) and the NFκB-DNA complex (black).

DNA binding by NFκB results in widespread changes in NFκB dynamics

To investigate the regions of NFκB that are affected by DNA-binding, we turned to HDXMS to monitor differences in amide exchange between free NFκB and the NFκB-DNA complex in both p50 (Figure 5.2) and p65 (Figure 5.3). As can be seen in Figure 5.2, the regions of p50 that exhibited increased amide exchange were localized to peptides 159-173 (1656.85, panel G), 215-225 (1142.54, panel J), and 283-298(1863.73, panel M); regions of p50 that showed decreased amide exchange upon DNA binding were localized to peptide 43-55 (1646.91, panel A), 97-221 (2681.41, panel C), 135-151 (1911.14, panel E), 235-248 (1478.71, panel K), 311-320 (1239.67, panel O). The regions of p65 that showed increased amide exchange in the NFκB-DNA complex included peptides 100-119 (306.09, Figure 5.3C), 133-147 (1807.91, panel E), 195-213 (2068.01, panel I), and 28 6-300 (1933.90, panel O). The p65 peptides that exhibited diminished exchange include peptides 23-34 (1502, panel A), 77-94 (2059.08, panel B), 120-132 (1517.81, panel D), 148-15 (1051.48, panel F), and 214-226 (1531.80, panel J).

The difference in deuterium uptake between the free NFκB and the NFκB-DNA complex were plotted on the NFκB structure (1VKX) (Figure 5.4). The regions of NFκB encapsulating the DNA underwent decreased exchange compared to free NFκB, whereas the periphery of NFκB showed increased amide exchange.
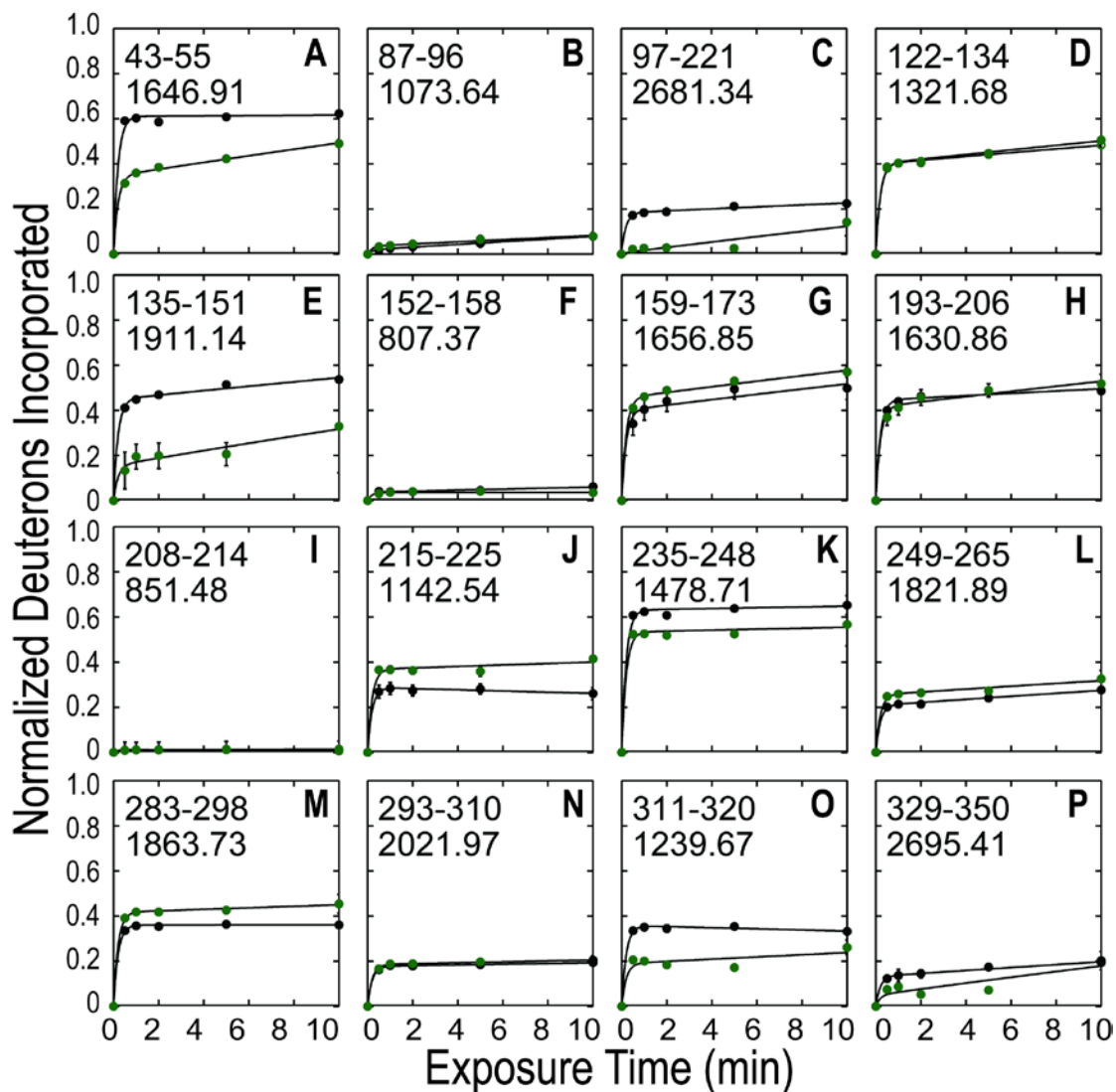
Figure 5.2. Amide H/D exchange plots of p50 peptides comparing free NFκB (●) with the NFκB-DNA complex (●). Regions of p50 that showed diminished amide exchange due to DNA binding are highlighted in peptides 43-55 (A), 97-221 (C), 135-151 (E), 235-248 (K), 311-320 (O); regions of p50 that underwent increased amide exchange due to DNA binding are highlighted in 159-173 (G), 215-225 (J) and 283-298 (M).
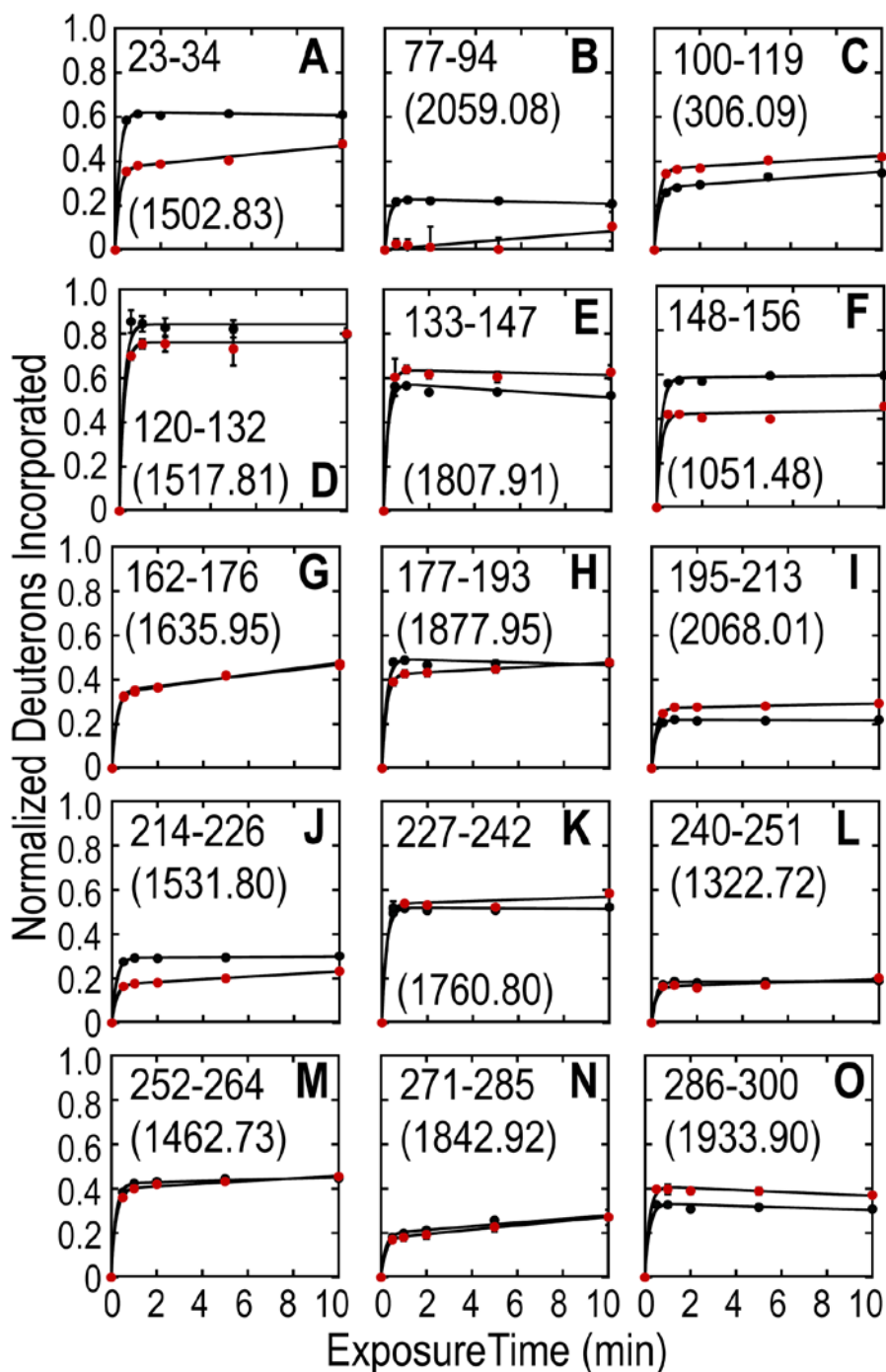
Figure 5.3. Amide H/D exchange plots of p65 peptides comparing free NFκB (●) with the NFκB-DNA complex (●). Regions of p65 that exhibited diminished amide exchange due to DNA binding are highlighted in peptides 23-34 (A), 77-94 (B), 120-132 (D), 148-15 (F), and 214-226 (J); regions of p65 that underwent increased amide exchange due to DNA binding are highlighted in peptides 100-119 (C), 133-147 (E), 195-213 (I), and 286-300 (O).
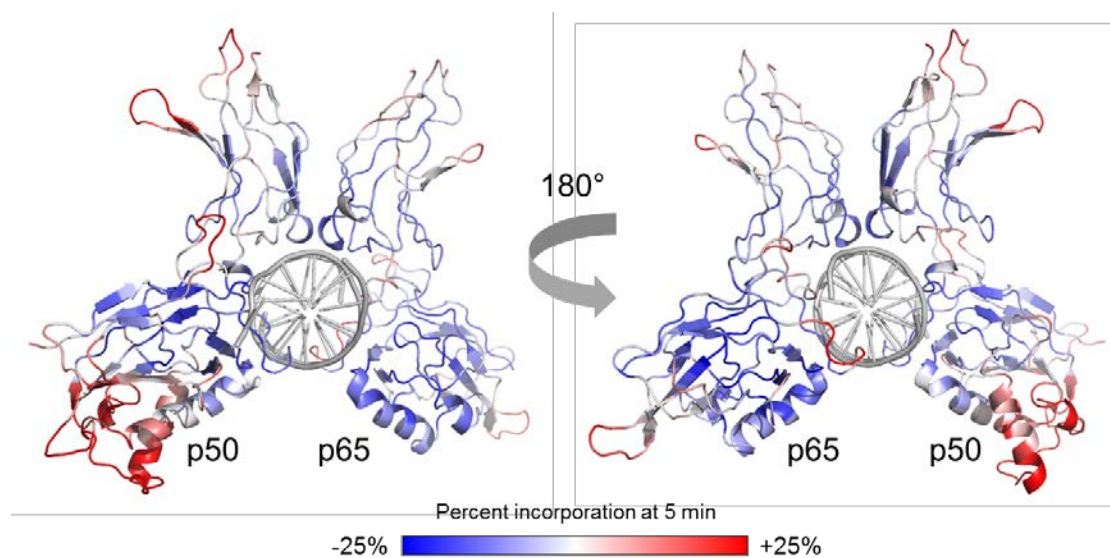
Figure 5.4. Amide exchange heat map comparison between free NFκB and the NFκB-DNA complex plotted on the NFκB structure (1VKX). Upon DNA-binding, the regions of NFκB enveloping DNA underwent less amide exchange than free NFκB (blue), whereas the periphery of NFκB exhibited increased amide exchange upon DNA binding when compared to free NFκB (red).

Discussion

By means of thermal denaturation and HDXMS, we have shown that the NFκB-DNA complex has increased stability compared to free NFκB, and the epicenter of this stability is the DNA binding site. In fact, many of the peptides that exhibited decreased amide exchange in NFκB upon DNA binding encompassed residues that are known to make direct contacts to the κB DNA sequence.[8, 9] For example, the p50 peptides 135-151 (1911.14) and 235-248 (1478.71) include the DNA-contacting residues K144 and K241, respectively. The p65 peptides 22-34 (1502.83), 120-132 (1517.81), and 214-226 (1531.80) include the DNA-contacting residues R33, K122/K123, and K218/K221, respectively.

The peptides that displayed increased amide exchange upon DNA binding were localized to the perimeter of the NFκB protein and include the p50 peptides 159-173 (1656.85), 215-225 (1142.54), and 283-298 (1863.73) and the p65 peptides 100-119 (306.09), 133-147 (1807.91), 195-213 (2068.01), and 286-300 (1933.90). In step with observations in Chapter 2, we observed an "accommodation" phenomenon wherein buttoning-down the DNA-binding domain of NFκB results in increased exchange along the fringes of NFκB.

Moving forward, we will study the effects of other NFκB binding partners (e.g., IκBα, IκBβ) as well as other NFκB constructs (i.e., dimerization domain $p50_{248-350}$/$p65_{190-321}$) in an effort to elucidate the relationship between NFκB dynamics, structure, and function.

Acknowledgements

Chapter 5, in full, is material in preparation for journal submission to which the dissertation author contributed equally with K. Ramsey. The material will be submitted for publication (**Dembinski, H.**, Ramsey, K., Komives, E.A. Global stabilization of NFκB upon IκBα and DNA binding).

References

1. Thanos, D., and Maniatis, T. (1992) The high mobility group protein HMGI(Y) is required for NFkB dependent virus induction of human IFN-beta gene, *Cell 71*, 777-789.

2. Urban, M. B., and Baeuerle, P. A. (1990) The 65-kD subunit of NFkB is a receptor for IkB and a modulator of DNA-binding specificity, *Genes Dev 4*, 1975-1984.

3. Bergqvist, S., Alverdi, V., Mengel, B., Hoffmann, A., Ghosh, G., and Komives, E. A. (2009) Kinetic enhancement of NF-kappaB•DNA dissociation by IkappaBalpha, *Proc. Nat. Acad. Sci. U.S.A. 106*, 19328-19333.

4. Oeckinghaus, A., and Ghosh, S. (2012) The NFkB Family of Transcription Factors and Its Regulation, *Cold Spring Harb. Symp. Perspect. Biol. 1*, 1-14.

5. Tsui, R., Kearns, J. D., Lynch, C., Vu, D., Ngo, K. A., Basak, S., Ghosh, G., and Hoffmann, A. (2015) IκBβ enhances the generation of the low-affinity NFκB/RelA homodimer., *Nat. Commun. 6*, 7068-7074.

6. Sue, S. C., Cervantes, C., Komives, E. A., and Dyson, H. J. (2008) Transfer of Flexibility between Ankyrin Repeats in IkappaBalpha upon Formation of the NF-kappaB Complex., *J. Mol. Biol. 380*, 917-931.

7. Wales, T. E., Fadgen, K. E., Gerhardt, G. C., and Engen, J. R. (2008) High-speed and high-resolution UPLC separation at zero degrees Celsius, *Anal. Chem. 80*, 6815–6820.

8. Chen, F. E., Huang, D. B., Chen, Y. Q., and Ghosh, G. (1998) Crystal structure of p50/p65 heterodimer of transcription factor NF-kappaB bound to DNA., *Nature. 391*, 410-413.

9.   Berkowitz, B., Huang, D. B., Chen-Park, F. E., Sigler, P. B., and Ghosh, G. (2002) The x-ray crystal structure of the NF-kappa B p50.p65 heterodimer bound to the interferon beta -kappa B site., *J. Biol. Chem. 277*, 24694-24700.